THE UNIVERSITY OF EDINBURGH

SCHOOL OF GEOSCIENCES

Photosynthetic response of the Antarctic moss species *Sanionia uncinata* (Hedw.) Loeske to varying light, water, and temperatures

BY

ALEX COLETY

in partial fulfilment of the requirement for the
Degree of BSc with Honours in
Ecological and Environmental Sciences

April 2024

Abstract

Antarctic vegetation is dominated by cryptogams, particularly mosses and lichens, which are resilient to extreme conditions. One key moss species in Maritime Antarctica is *Sanionia uncinata*, a hydric, carpet-forming species with a global distribution. *S. uncinata* is a key part of the maritime Antarctic ecosystem and a habitat for diverse bacterial, fungal, and invertebrate communities. A few previous studies have investigated the light, water, and temperature preferences of *S. uncinata* but their conclusions are inconsistent. As *S. uncinata* is a key species in a region that is experiencing high levels of warming, it is increasingly important to understand its physiological traits in order to predict changes in the ecosystem. In this study, I investigate the photosynthetic response of *S. uncinata* to light, water, and temperature variation. The first component is a field study under ambient conditions at Robert Island, Maritime Antarctica (62°24'S, 59°30'W). This is followed by a laboratory study under experimental conditions. Key findings were that *S. uncinata* is rarely light limited in the field, tolerant of intense light, and is equally productive over a broad range of temperatures. Water responses were somewhat unclear between field and lab results, but ultimately showed that water is the primary limiting factor for *S. uncinata* at Robert Island. Taken together, these results suggest that future increases in rainfall and increased mean temperatures in Maritime Antarctica will neutrally or positively impact *S. uncinata* productivity.

Table of Contents

Acknowledgements

First and foremost, I'd like to thank Dr Claudia Colesie for her guidance, ideas, and advice while supervising this project. I would also like to thank her PhD student, Charlotte Walshaw, who collected the field data I've presented in this dissertation and the sample I used in the laboratory component. Charlotte has been wonderfully helpful in providing her field notes, details about her methodology, and general advice over the last few months. I would also like to acknowledge the advice and feedback I've received from Dr Jamie Weir on various details and my approach for reporting and comparing regressions.

Finally, a big thank you to my obligatory proofreaders, my parents, who braved the earlier versions of this dissertation. Extra thanks additionally go to Heather Young for her proofreading and moral support.

Abbreviations

CI: Confidence interval

CO_2: Carbon dioxide

dCO_2 : Difference in CO_2 concentration between air entering and exiting the sample cuvette

DR: Dark respiration

IRGA: Infrared gas analyser

LCP: Light compensation point

LSP: Light saturation point

NLS: Nonlinear least squares

NP: Net photosynthesis

NP_{max}: Maximum net photosynthesis

PPFD: Photosynthetic photon flux density

ppm: Parts per million

Q_{10}: Temperature coefficient of respiration

QR: Quadratic regression

WC: Water content

WC_{opt}: Optimum water content

WCP: Water compensation point

1. Introduction

Antarctic flora is dominated by cryptogams—particularly mosses and lichens—due to an extreme climate which limits the vegetation that can survive there. Vegetation that does persist must contend with short growing seasons, continuous light in the summer, limited water, low temperatures, a highly seasonal climate, and frequent strong winds (Robinson et al., 2003; Silva et al., 2018). Microhabitat temperatures are frequently at the minimum threshold for biological processes to occur (Convey, 2006). Generally, Antarctic vegetation copes with cold temperatures by having low stature, compact growth form, phenotypic plasticity, and communal aggregation (Block et al., 2009). Compact growth such as that in mosses improves both heat and water retention, helping vegetation to withstand cold and dry periods (Block et al., 2009). Within Antarctica, the maritime region has a relatively milder climate and hosts the most flora with 100-115 moss species, 350 lichen species, 27 liverwort species, and 2 phanerogam species (Peat et al., 2007).

Generally, changes in temperature, water, solar radiation, and atmospheric carbon dioxide (CO_2) levels are expected to affect Antarctic terrestrial organisms (Convey, 2006; Royles et al., 2012). Drivers of Antarctic climate variability are complex (King et al., 2003; Turner et al., 2016), but it is well known that polar regions including Maritime Antarctica are experiencing warming faster than other areas of the world (Bromwich et al., 2013; Turner et al., 2019; Clem et al., 2020; Rantanen et al., 2022). Projected changes to the Antarctic climate are expected to both enhance (ex. extended growing season, CO_2 fertilization) and limit (ex. increased erosion and disturbance) vegetation growth in the future (Royles et al., 2012; Royles and Griffiths, 2015). Currently, the northwestern region of the Antarctic Peninsula sees 55 to 105 days of liquid precipitation yearly (Vignon et al., 2021). This region is expected to experience an overall increase in rainfall by the end of the 21st century, though some local areas may see decreases in liquid precipitation. The projected increase in rainfall is related to an expected increase in days with mean temperatures above 0 °C (Vignon et al., 2021). Higher mean temperatures are also expected to alter vegetation growth rates (Royles et al., 2012). Changes in meltwater are expected to alter dynamics as well because many patches of vegetation are reliant on meltwater rather than precipitation as a primary water source. Increased temperatures may cause greater snowmelt earlier in the growing season, causing water-limiting conditions by the end of the season after the source has been depleted (Robinson et al., 2003; Convey, 2006).

Modelling studies have produced predictions for large-scale atmospheric and circulation changes around the Antarctic. Smaller, more local changes are also important to examine when considering vegetation. Microhabitat conditions become increasingly important to determining vegetation distributions at high latitudes (Green et al., 2011). Snow cover can be highly variable on small scales in Maritime Antarctica and the extent of snow cover affects vegetation dynamics (Tarca et al., 2022). Soil temperatures are also important to the biology of polar systems. They

vary greatly over landscape scales because they are determined by air temperature, albedo, radiative forcing, and ground insulation (Convey et al., 2018). Water availability at smaller, microhabitat scales is highly variable and critical for determining distributions of life in Antarctica (Kennedy, 1993; Schlensog et al., 2013). Predicted increases in liquid precipitation could increase bryophyte production in areas that are currently water limited. Conversely, Royles et al. (2012) have shown that past climatic changes which decreased bryophyte surface water, such as higher temperatures and wind speeds, had actually led to higher carbon assimilation rates rather than lower. This is because excess water on bryophyte surfaces limits the rate at which they can absorb CO_2 from the atmosphere. Overall, the factors that influence vegetation dynamics are complex, subject to change, and difficult to predict.

Despite the harsh and variable conditions, there are 116 recorded moss species present at latitudes higher than 60 °S (Câmara et al., 2021). As a dominant flora type, mosses play important roles in Antarctic ecosystems. Moss cover is important for insulating soil and permafrost (Prather et al., 2019; Hrbáček et al., 2020). Moss presence cools the ground surface in spring and summer by up to 6.9 °C, reducing both the mean temperature and the amplitude of temperature fluctuations (Hrbáček et al., 2020). This in turn affects ground freeze-thaw cycles which influences water availability in the soil (Convey et al., 2018). Moss cover also affected soil by increasing soil water retention (Prather et al., 2019). Vegetation cover also influences the net carbon exchange between soil and atmosphere, with a species-specific effect (Mendonça et al., 2011; Cannone et al., 2012).

Mosses excel in two key strategies for thriving in the Antarctic climate. They are able to cope with long periods of poor growing conditions and are equally able to respond quickly when favourable conditions arise (Block et al., 2009). Mosses can suspend their metabolism when water is not sufficiently available, a key limitation in Antarctic ecosystems (Silva et al., 2018). In a dehydrated state, they can withstand stressful conditions but quickly resume metabolic activity when rehydrated. Multiple studies have also demonstrated the ability of polar mosses to respond rapidly to changing environmental conditions. *Bryum argenteum* var. *muticum* net photosynthesis (NP) acclimates to experimentally increased temperatures within just seven days (Gemal et al., 2022). The same species has shown plasticity to light conditions. Schroeter et al. (2012) investigated acclimation between shade and sun conditions and found that a shade-adapted form of *B. argenteum* was able to acclimate to high light conditions within five days. The individual adapted by growing new shoots with increased chlorophyll content and heightened light saturation point (LSP; Schroeter et al., 2012). Additionally, the cosmopolitan moss *Ceratodon purpureus* has shown distinct physiological strategies at different habitats in the continental and maritime Antarctic, as well as in South Africa (Beltrán-Sanz et al., 2023). The study found physiological variation in respiration rates, photosynthetic efficiency, thermal optimum, and shade- versus sun-adapted traits (Beltrán-Sanz et al., 2023). Generally, mosses

also benefit from being able to reproduce asexually when environmental conditions are unfavourable, and sexually when conditions are less stressful (Smith and Convey, 2002; Block et al., 2009). Ability to adjust quickly to changing conditions is advantageous when growing in highly variable environments.

Despite being a remote location, there is a good existing body of knowledge surrounding Antarctic flora, particularly in maritime locations (Peat et al., 2007). Moss distributions and characteristics have been used to understand the past climate, and monitoring can be used to explore current climatic changes in Antarctica (Royles and Griffiths, 2015). For example, Royles et al. (2012) found Antarctic moss growth rates from 1980 to 1995 to be higher than was expected from CO_2 fertilization—this was likely due to high temperatures and longer growing season. In order to best understand how vegetation changes might reflect climatic changes, there is a need for baseline knowledge about key species.

One such key species is *Sanionia uncinata* (Hedw.) Loeske. *S. uncinata* is a predominant species on the islands of the maritime Antarctic (Longton, 1967; Putzke et al., 2015; Silva et al., 2018). The species can be found globally and persists in both Arctic and Antarctic environments. It is a fast colonizer and can form vast moss carpets (Longton, 1967; Putzke et al., 2020). *S. uncinata* has been used to monitor the presence of persistent organic pollutants in the atmosphere (Wu et al., 2014), study lead input into the Antarctic environment (Choi et al., 2022), and explore UV protective properties for potential cosmetic use (da Silva Fernandes et al., 2019). In Maritime Antarctica, *S. uncinata* hosts diverse communities of endophytic bacteria (Park et al., 2013), protozoans (Mieczan and Adamczuk, 2015), other microorganisms, and invertebrates (Prather et al., 2019). Soils underneath *S. uncinata* also demonstrate higher fungal and bacterial abundance than bare ground (Benavent-González et al., 2018). Species-specific effects of vegetative cover on soil properties show that soils beneath *S. uncinata* have increased soil nutrient content, and other altered soil properties, when compared to bare soils and other Antarctic moss and lichen species (Benavent-González et al., 2018). Vegetation communities dominated by *S. uncinata* show high net ecosystem exchange and ecosystem respiration rates when compared to other types of vegetation (Cannone et al., 2012).

Like other mosses, *S. uncinata* NP is primarily determined by light availability, water content (WC), and temperature. Ueno et al. (2006) found that *S. uncinata* colonies in the high Arctic have variable light responses depending on water conditions in their environment. Constantly wet and sunny environments hosted colonies that photosynthesized more effectively at high light conditions, while dry environments hosted colonies that photosynthesized more effectively under the low light conditions that are characteristic of rainy and overcast days (Ueno et al., 2006). Summer light in the Antarctic can be intense, but *S. uncinata* is highly resistant to photoinhibition (Orekhova et al., 2021). Orekhova et al. (2021) found that the photosynthetic recovery was fast after *S. uncinata* samples experienced photoinhibition under experimental

conditions. The species is additionally tolerant of ambient UV-B exposure, though high experimental exposure does cause damage (Lud et al., 2003).

S. uncinata is primarily a hydric species (Fowbert, 1996). Pizarro et al. (2019) examined the desiccation tolerance of *S. uncinata* and determined that desiccation affected both photosynthetic and respiratory activity, though the impact on photosynthesis was more dramatic. In contrast, Uchida et al. (2002) determined that respiration was not significantly impacted by WC in *S. uncinata*. There has also been disagreement about the water compensation point (WCP)—Uchida et al. (2002) found no photosynthesis in WC under 40% but Nakatsubo (2002) found this point to be much higher at 160%.

As a species found in cold environments, *S. uncinata* relies on low temperatures to maintain and positive carbon balance (Nakatsubo, 2002). However, Davey and Rothery (1997) found *S. uncinata* to be operating under less-than-optimal temperatures and suggested that optimal temperatures for NP were above 15 °C. Perera-Castro et al. (2020) similarly found *S. uncinata* in the Antarctic to have an optimum temperature of 24 °C. Despite photosynthesizing at sub-optimal temperatures, limited respiration at low temperatures allows *S. uncinata* to maintain a positive carbon balance (Perera-Castro et al., 2020). In contrast, both Nakatsubo (2002) and Uchida et al. (2002) found relatively constant NP rates between temperatures 5 to 15 °C and 7 to 23 °C, respectively. Despite finding a relatively constant NP rate, Nakatsubo (2002) developed a model which indicated that a 5 °C increase in temperature would lead to a 63% decline in *S. uncinata* colony carbon gain and agreed with Perera-Castro et al. (2020) that *S. uncinata* maintains a positive carbon balance by having limited respiration at low temperatures. The studies have given directly contradicting results on the temperature preferences of *S. uncinata*, and this point requires further clarity.

Because there are relatively few studies of *S. uncinata*'s physiological preferences, is unsurprising that there are disagreements among those few that exist. This is exacerbated by the existing studies having taken place in different geographic areas, meaning there is limited location-specific information to draw upon. Knowing that mosses rely primarily on light, water, and temperature conditions to determine their growth, and knowing that these conditions are subject to change in a warming and variable Antarctic climate, it is increasingly important to understand how moss productivity responds to these factors. As such, this study aimed to add to the knowledge about *S. uncinata* by examining its photosynthetic response under various light, water, and temperature scenarios in both laboratory and field settings. To do this, I assessed (1) the environmental conditions that *S. uncinata* is exposed to on Robert Island during the summer, (2) what *S. uncinata*'s photosynthetic response to these conditions is *in situ*, (3) how *S. uncinata* responds to light, water, and temperature conditions beyond those experienced *in situ*, as determined in a laboratory experiment, and (4) whether field and laboratory photosynthetic responses were similar.

I hypothesised that *S. uncinata* would have sufficient light for photosynthesis during the field season, with light compensation points (LCP) between 50 and 100 µmol photons m^{-2} s^{-1} and LSP between 450 and 900 µmol photons m^{-2} s^{-1} (Figure 1A; Nakatsubo, 2002; Uchida et al., 2002; Ueno et al., 2006). I did not expect to see evidence of photoinhibition under ambient conditions or at light intensities used in the lab.

Because *S. uncinata* is hydric, I hypothesised that WC would significantly influence both photosynthesis and respiration rates (Figure 1B). The maritime Antarctic is relatively wet, so I did not expect *S. uncinata* to be water limited in the field. Based on previous studies, I expected the optimal water content (WC_{opt}) to be between 270% and 690% (Nakatsubo, 2002; Uchida et al., 2002). I also expected dark respiration (DR) to have a more modest response to WC than photosynthesis.

For temperature, I hypothesised that *S. uncinata* in the field would colder than its optimum and that the lab experiment would show optimal temperatures from 15 to 20 °C (Figure 1C; Davey and Rothery, 1997; Perera-Castro et al., 2020). I expected DR to increase with increasing temperature, with an Q_{10} value between 2.0 to 3.5 (Davet and Rothery, 1997; Nakatsubo, 2002; Uchida et al., 2002). When comparing regressions for field versus laboratory data at 5 °C, I expected to find that the regressions were comparable, with higher noise in field measurements (Figure 1D).

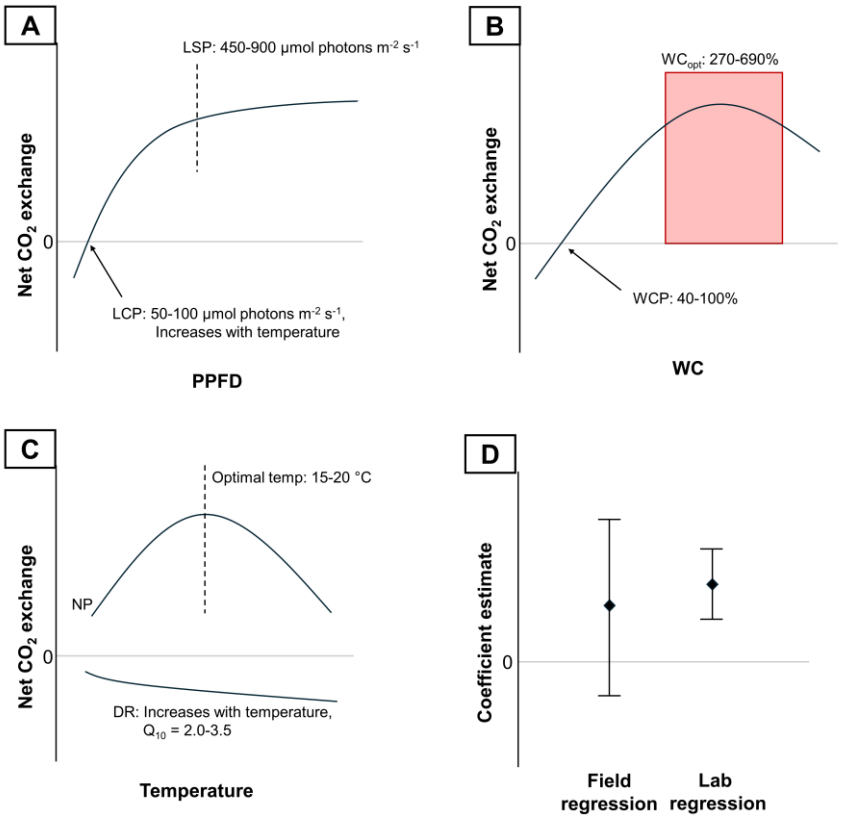

Figure 1. Graphical representation of hypotheses. (A) shows expected light response, (B) shows expected water response, (C) shows expected temperature response, and (D) shows how regression coefficients may relate.

2. Methods

2.1. Study site

The field component took place at the Coppermine Peninsula on Robert Island, South Shetland Islands, Maritime Antarctica (62°24'S, 59°30'W; Figure 2). The South Shetland Islands are approximately 100 km northwest of the Antarctic Peninsula, between the Drake Passage and Bransfield Straight. Robert Island itself is situated approximately 70 km southwest of King George Island, the largest of the South Shetland Islands. Robert Island arose in the Jurassic or early Cretaceous period and is composed primarily of igneous and volcaniclastic rocks (Smellie et al., 1984; Secretariat of the Antarctic Treaty, 2012). It is largely covered by a single ice cap and its largest outcrop is the Coppermine Peninsula (Secretariat of the Antarctic Treaty, 2012; Kandemir et al., 2023). The Coppermine Peninsula is an Antarctic Specially Protected Area (ASPA no. 112) due to its biologically rich floral and faunal colonies, particularly a 1.5 ha moss carpet (Secretariat of the Antarctic Treaty, 2012). It hosts one of the two vascular plant species present in Antarctica, 23 moss species, two liverworts, two algae, and 27 lichens. 11 species of birds and four seal species are also present (Secretariat of the Antarctic Treaty, 2012).

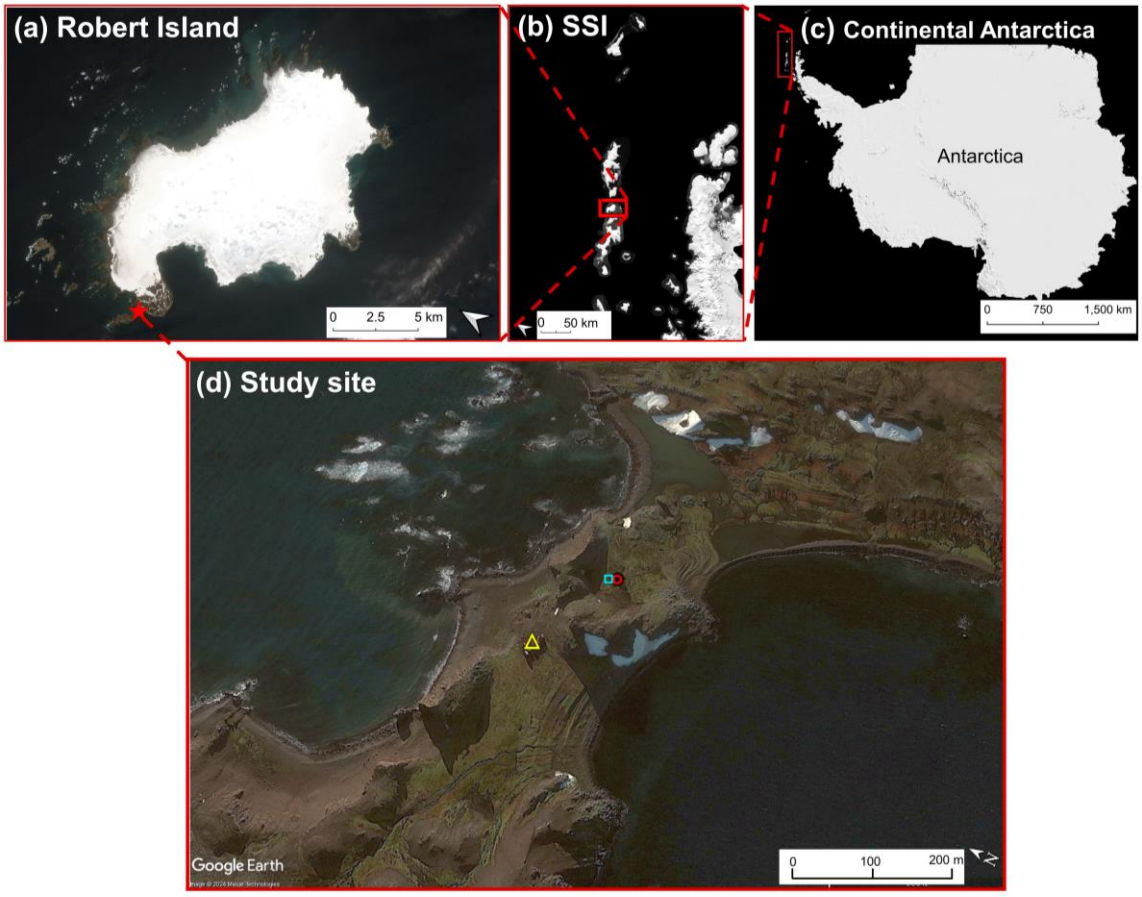

Figure 2. Study location relative to continental Antarctica, South Shetland Islands (SSI), and Robert Island. In (d), yellow triangle shows the Rispatrón base, red circle shows the original location of the field sample of *S. uncinata*, and blue square shows the lab sample of *S. uncinata*. Images generated with Google Earth Engine (v7.3.6.9796; Google Earth, 2024) and QGIS (v3.36.1; QGIS, 2024) using the Norwegian Polar Institute's Quantarctica (Matsuoka et al., 2018; Bindschadler et al., 2008). Image (a) made with imagery optimized by Charlotte Walshaw.

The South Shetland Islands experience high mean temperatures due to their relatively northern position and warm north-westerly winds (Mayewski et al., 2009; Turner et al., 2019). There is considerable inter-annual variability in mean temperatures, though this is lesser than along the western side of the Antarctic Peninsula (Turner et al., 2019). In terms of precipitation, Maritime Antarctica receives about 25 to 100 cm of water-equivalent annually (Kennedy, 1993). This precipitation falls mainly as snow, but rain can be fairly frequent during the summer (Schroeter et al., 1995).

Bright and sunny days in the maritime Antarctic can reach PPFDs (photosynthetic photon flux density) of around 1560 µmol photons m^{-2} s^{-1} while overcast and rainy days average about 300 µmol photons m^{-2} s^{-1} (Schroeter et al., 1995). PPFDs above 700 µmol photons m^{-2} s^{-1} generally occur above midday and are restricted to short periods (Davey and Rothery, 1996). There is frequent cloud cover, with mean daily sun duration during the summer ranging from 2 to 5.5 hours (Longton, 1967). January and February receive 6 and 9 hours of darkness daily, respectively (Schroeter et al., 1995).

2.2 Study species

S. uncinata (Hedw.) Loeske was selected because of its prevalence at Robert Island. It is abundant throughout Maritime Antarctica and forms moss carpets (Longton, 1967). The species has a global distribution, from temperate regions to the Arctic and Antarctic, and can be found at many altitudes (Hedenäs, 2003). *S. uncinata* persists in diverse habitats, from forests to open areas (Longton, 1967; Hedenäs, 2003). It is somewhat tolerant of dry conditions, but is primarily a hydric species (Longton, 1967; Fowbert, 1996).

2.3 Field data collection

A PhD student collected field data from 5 January 2023 to 16 February 2023. The PhD student selected the sample used for *in situ* measurement based on its proximity to the Risopatrón base, where she took CO_2 exchange measurements, and for its health, based on visual observation.

After identifying the field sample, she removed it from its substrate and secured it to a nonreactive metal basket using fishing line. When taking measurements, she brought the sample to a Scott polar tent outside of the Risopatrón base, weighed the sample, and then took gas exchange measurements at ambient conditions using a portable infrared gas analyser (IRGA; GFS-3000, Heinz Walz GmBH, Effeltrich, Germany) and gas exchange cuvette (3010-GWK1, Heinz Walz GmbH, Effeltrich, Germany). After placing the sample in the cuvette, the

PhD student waited for the difference in CO_2 between air entering and exiting the cuvette (dCO_2) to stabilise to within 0.5 ppm before recording datapoints. She returned the sample to its original location between measurements so that it would be exposed to regular field conditions. A weather station (HOBO Micro Station H21-USB, Onset Computer Corporation, Massachusetts, USA) recorded additional environmental parameters, including PPFD and air temperature.

Over the field season she took approximately three measurements per day from one *S. uncinata* sample. The full three measurements were not always possible due to weather conditions. Constraints of the IRGA meant that she could not determine CO_2 exchange rates during periods of high wind or rain. Excepting these conditions, she collected data from a range of weather conditions to produce a dataset representative of the environment.

The PhD student used one *S. uncinata* sample for field measurements. At the end of the field season, she collected seven additional samples for laboratory use. She air dried the field and additional samples before they were transported, frozen at -20 °C, to Edinburgh, United Kingdom. In Edinburgh, the samples were stored frozen at -20 °C.

2.4 Laboratory data collection

I collected laboratory data between 12 February and 5 March 2024. I measured CO_2 exchange with the same IRGA and cuvette as was used for field measurements. I additionally used an LED panel to control the PPFD (LED-Panel RGBW-L084, Heinz Walz GmbH, Effeltrich, Germany). Throughout all measurements, IRGA airflow and cuvette fan settings were the same as for field measurements. Before recording each measurement on the IRGA, I ensured that dCO_2 had stabilized to within 0.5 ppm for at least 2 consecutive minutes. When measuring DR, I covered the cuvette with an opaque, black fabric. I obtained sample weight with a digital scale with accuracy within 0.1 mg (HR-250A, A&D Company Ltd., Tokyo, Japan).

2.4.1. Sample thawing and storage

I removed one sample from the freezer and placed it in an airtight plastic container in a refrigerator to defrost in the dark at 4 °C for 72 hours. After 24 hours, I saturated the sample with water collected from the Braid Burn, a local stream. Stream water was used due to the presence of chlorine in tap water, which could have damaged the sample. Once the sample had thawed, I attached it to a nonreactive metal basket using fishing line.

Between days of data collection, I stored the sample in an airtight, plastic container in the refrigerator at 4 °C to prevent it from acclimating to experimental conditions. The sample was stored as dry as possible to prevent fungal and bacterial growth.

I additionally thawed the original field sample before oven drying it to obtain its dry weight (see 2.4.5). I did this in the same manner as thawing the lab sample, however I did not saturate it after 24 hours.

2.4.2. Light response curves

I measured light response curves at 5, 10, 15, and 20 ± 1 °C. To prevent acclimation to a warming or cooling temperature trend, I collected data first at 15 °C, then 5, 20, and 10 °C. I measured CO_2 exchange at PPFDs 0, 50, 100, 200, 400, 800, and 1200 ± 50 µmol photons m^{-2} s^{-1}, starting at 0 µmol photons m^{-2} s^{-1} and progressively increasing the PPFD. I moistened the sample to its approximated WC_{opt}, 110 ± 20%, and checked sample weight at the beginning, middle, and end of each light response curve to ensure the WC remained in that range. Air entering the cuvette had a relative humidity of 80% to prevent the sample from drying.

2.4.3. Desiccation curve

I measured desiccation curves at 5, 10, 15, and 20 ± 1 °C, in the same order as for the light response curves. Throughout the desiccation cycle, the PPFD was 550 ± 60 µmol photons m^{-2} s^{-1} for NP measurements. The air entering the cuvette had a relative humidity of 50% to aid in sample drying.

I saturated the sample thoroughly with stream water, shaking it gently to remove excess water on the moss surface. After the sample was saturated, I recorded its weight and placed it into the cuvette. I took two measurements at a time. First, I covered the cuvette with an opaque, black fabric and recorded DR. Then I removed the cloth cover and turned on the light panel to measure NP. After the paired DR and NP measurements were finished, I removed the sample from the cuvette and recorded its weight. I allowed the sample to air dry for 15 to 30 minutes before placing back into the cuvette and repeating the process. I repeated this until the sample weight was near-constant, indicating a very low water content.

2.4.4. Temperature response

I did not directly measure temperature response curves. I used data generated by the above measurements to interpret the temperature response.

2.4.5. Drying samples

I oven-dried both the lab and field *S. uncinata* samples. I first obtained their saturated weight by soaking them thoroughly with stream water and shaking off the excess until no drops ran off. I weighed each sample with metal baskets and fishing line still attached, then removed the baskets and fishing line and weighed them separately. I could then subtract basket and fishing line weights from the weights recorded during field and lab measurements. I allowed samples to air dry and then finished drying them in a drying oven (Ufb 400, Memmert GmbH + Co.KG,

Schwabach, Germany) at 60 °C for 72 hours. I then weighed the samples again for their dry weight.

2.5 Quality control and statistical methods

I completed analysis using R (v4.1.1; R Core Team, 2021) and RStudio (v2023.06.1; Posit team, 2023). Code and raw data are available in Appendix 4. Key analytical packages were tidyverse, including ggplot2 for data visualisation (v2.0.0; Wickham et al., 2019), nlstools (v2.1.0; Baty et al., 2015), broom (v1.0.5; Robinson et al., 2023), and rootSolve (v1.8.2.4; Soetaert, 2009). I used ImageJ to determine sample surface area (Schneider et al., 2012).

I determined NP rates based on area rather than per unit dry weight or chlorophyll concentration. This was to be able to directly compare with field data and to keep samples intact for further study. Additionally, measures of NP in terms of dry weight are affected by the amount of non-photosynthetic material included (Davey and Rothery, 1997).

When reporting statistics, I indicate the number of data points used to generate the statistics as *n*. It is important to note that these data points are repeat measures on a single sample (one sample for field data and one sample for lab data), rather than fully independent points.

2.5.1. NP and DR calculations

The IRGA (Figure 3) calculated CO_2 assimilation rate using the following equation from Caemmerer and Farquhar (1981):

$$A = u_e * \frac{(c_e - c_o)}{LA} - E * c_o$$

A = assimilation rate (μmol CO_2 m^{-2} s^{-1})
u_e = molar flow rate at cuvette inlet (μmol s^{-1})
c_e = CO_2 mole fraction at cuvette inlet (ppm)
c_o = CO_2 mole fraction at cuvette outlet (ppm)
LA = leaf area (cm^2)
E = transpiration rate (mmol m^{-2} s^{-1})

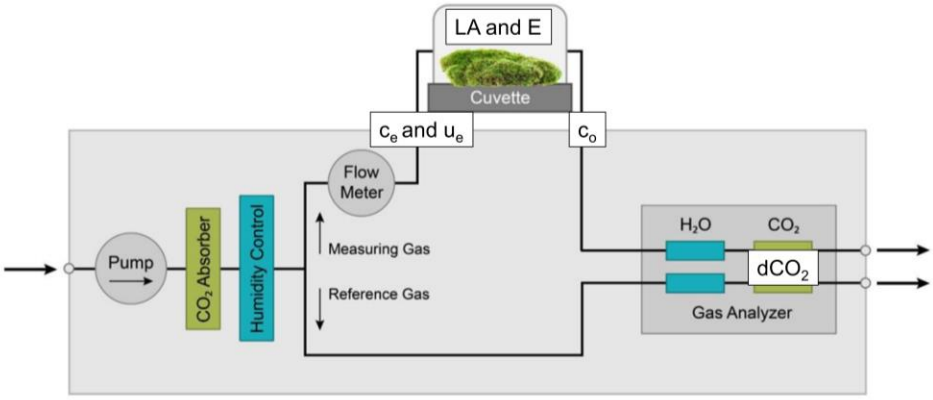

Figure 3. Schematic of IRGA function with key parameters for equations. Adapted from Gemal (2021) and the Heinz Walz GmbH GFS-3000 operation manual.

2.5.2. Determining light response

I fit a nonlinear least squares (NLS) asymptotic exponential regression to the light response data (Uchida et al., 2002; Ueno et al., 2006). I used the following formula, calculating coefficients for each temperature:

$$NP_{(PPFD)} = a + (b - a) * \ e^{-e^{c} * PPFD}$$

$a =$ estimated asymptote
$b =$ y-intercept
$c =$ natural log of the rate constant

For field data, I included data points where temperature was 4.5 ± 1.5 °C and WC was greater than the WCP, 124%. There were only two field data points at WC_{opt}, hence the inclusion of all data above the WCP. For the lab data, I grouped data by temperature (5, 10, 15, and 20 ± 1 °C) and generated a best-fit regression at each temperature. I assessed all models with model summaries and diagnostic plots. I do not report NLS p-values because they were not available for the overall model, only for individual model coefficients. Further details of model outputs for each regression are available in Appendix 1. To assess NLS model fit, I used the following pseudo-R^2 recommended by Schabenberger and Pierce (2002):

$$pseudo\ R^2 = 1 - \frac{SS_{res}}{SS_{tot}}$$

$SS_{res} =$ regression sum of squares
$SS_{tot} =$ total sum of squares

After confirming suitability of the models, I used the regressions to calculate the light compensation point (LCP) and LSP at each temperature. LCP is the PPFD at which NP is 0 μmol CO_2 m^{-2} s^{-1} and LSP is the PPFD at which NP reaches 90% of its maximum.

2.5.3. Determining WCP and WC_{opt}

I first used weight to calculate sample WC as a percent of dry weight, as follows:

$$WC(\%) = \frac{([fresh\ weight - basket\ weight] - dry\ weight)}{dry\ weight} * 100$$

I then fit a quadratic regression (QR) to the field and lab data separately using the following equation:

$$NP_{(WC)} = a + b(WC) + c(WC)^2$$

For field data, I included data at which temperature was 4.5 ± 1.5 °C and PPFD was greater than 480 µmol photons m^{-2} s^{-1}. This ensured that all included data points were above the LSP. I confined values to this temperature range because of a presumed interaction between temperature and WC to determine NP (Uchida et al., 2002). For lab data, I grouped the data by temperature (5, 10, 15, and 20 ± 1 °C) and then fit a QR at each temperature due to the presumed interaction between WC and temperature to determine NP. I also fit a QR to DR measurements at each temperature for lab data. Field data did not include DR measurements. I assessed each model using model summaries and diagnostic plots.

Using the best-fit regressions, I calculated the WCP and WC_{opt} for field data and at each temperature for lab data. The WCP was the WC at which NP was equal to 0 µmol CO_2 m^{-2} s^{-1}. WC_{opt} was the WC at which the sample reached maximum NP (NP_{max}).

2.5.4. Determining temperature response

I determined the temperature response curve with lab data generated from desiccation and light response measurements. I fitted a QR to the data in the same way as with the water content, using temperature as a variable instead of WC (Nakatsubo, 2002). I filtered data to include measurements at WC_{opt} and PPFDs 0 and 550 ± 60 µmol photons m^{-2} s^{-1}. I assessed fit using model summaries and diagnostic plots. Using the QR at a PPFD of 0 µmol photons m^{-2} s^{-1}, I calculated the Q_{10} value.

2.5.5. Comparing field versus laboratory regressions

I compared regressions fitted to field data and laboratory data for light responses and desiccation curves. This was to see whether responses to environmental variables were similar between the lab and field. I used the laboratory data where temperature was 5 ± 1 °C, as this was most similar to the data from field conditions which were 4.5 ± 1.5 °C. I plotted the coefficient and error bars using t-based 95% confidence intervals (CI) for the light response

curves. For desiccation curves, I plotted the coefficient with error bars that were two standard errors above and below the coefficient.

3. Results

A PhD student collected 41 measurements of *S. uncinata* CO_2 exchange at ambient conditions from a single sample, from 5 January 2023 to 16 February 2023. She collected additional data including ambient light level, sample WC, and air temperature.

3.1. Climatic conditions at Robert Island

3.1.1. Light intensity

Over the measurement period, the mean PPFD was 949 µmol photons m^{-2} s^{-1}. The minimum PPFD was 194 µmol photons m^{-2} s^{-1} and the maximum was 1999 µmol photons m^{-2} s^{-1}. Of 34 weather station light measurements, 34 (100%) were above the LCP for *S. uncinata* and 27 (79%) were over the LSP, as determined by the lab data at 5 °C (Figure 4A; see 3.3.1).

3.1.2. Water content

The mean sample WC was 180%. Minimum WC was 114% and maximum WC was 310%. Of 41 measurements, WC was above the WCP for 38 measurements (93%) and within the WC_{opt} range for 2 measurements (5%), as determined by a regression fitted to field data (Figure 4B; see 3.2.2).

3.1.3. Air temperature

The mean air temperature was 4.1 °C. Air temperature ranged from 2.2 to 6.1 °C (Figure 4C).

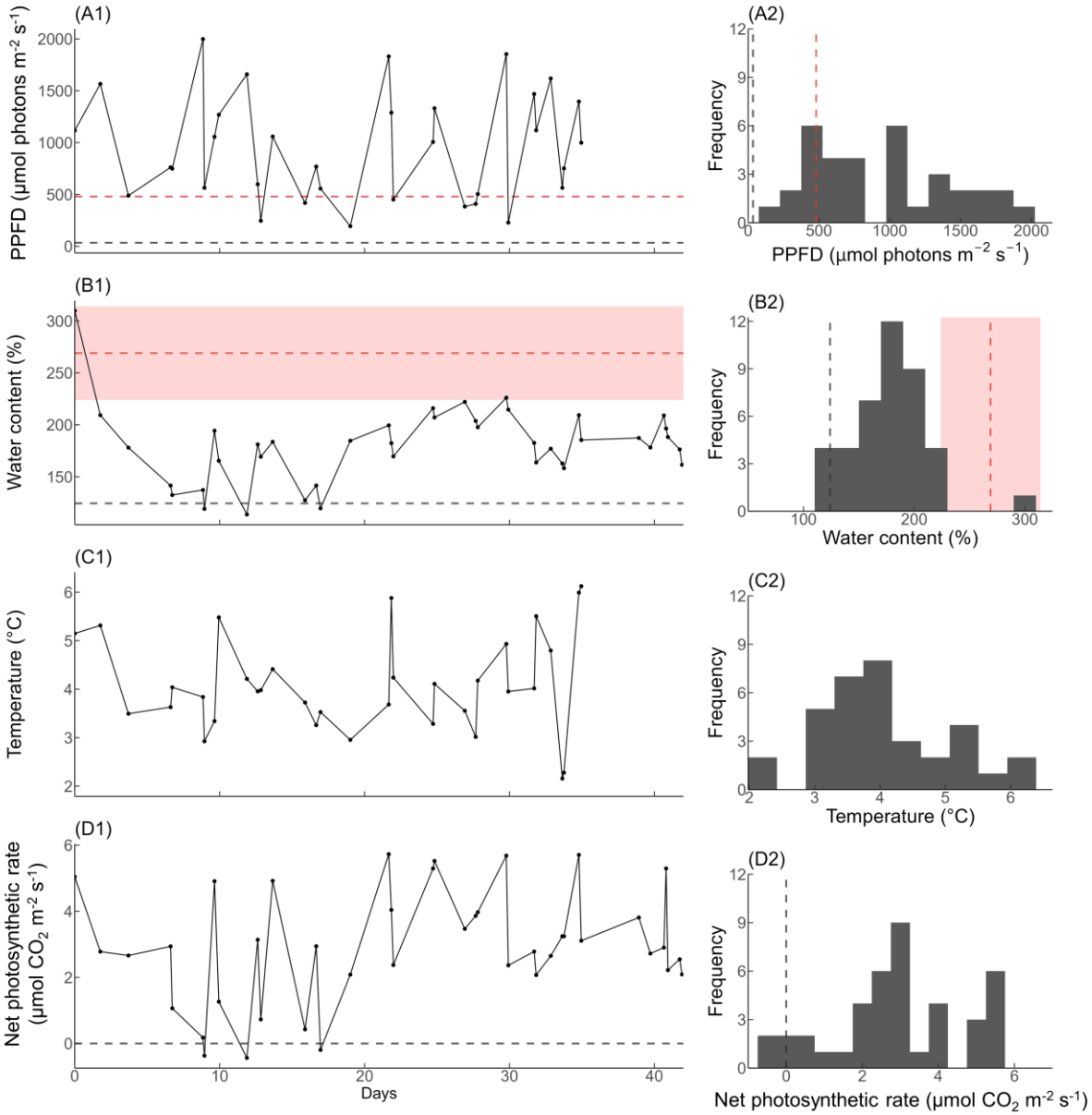

Figure 4. Timeseries of environmental conditions experienced at Robert Island from 5 January 2023 to 16 February 2023 (left) and frequency of conditions (right). Plots A1 and C1 show fewer days of data due to weather station data not being available for those days. For A1 and A2, red dashed line indicates the LSP (480 µmol photons m^{-2} s^{-1}) and black dashed line indicates the LCP (34 µmol photons m^{-2} s^{-1}), both as calculated from laboratory data. For B1 and B2, red dashed line with red box indicates the WC_{opt} range (269 ± 45%) and black dashed line indicates WCP (124%) as calculated from field measurements. For D1 and D2, black dashed line is NP = 0 µmol CO_2 m^{-2} s^{-1} .

3.2. Photosynthetic response *in situ*

The mean NP was 2.95 µmol CO_2 m^{-2} s^{-1}. NP ranged from -0.44 to 5.73 µmol CO_2 m^{-2} s^{-1}. NP was positive (P > R) for 38 measurements (93%) and negative (R > P) for 3 (7%; Figure 4D). NP_{max} occurred when PPFD was 1418 µmol photons m^{-2} s^{-1}, temperature was 3.7 °C, and WC was 200%.

3.2.1. Light response curves

There was no clear light response in the field (NLS, n = 27, pseudo-R^2 = 0.167; Figure 5). Data included to determine light response had temperatures of 4.5 ± 1.5 °C and WC greater than 124%.

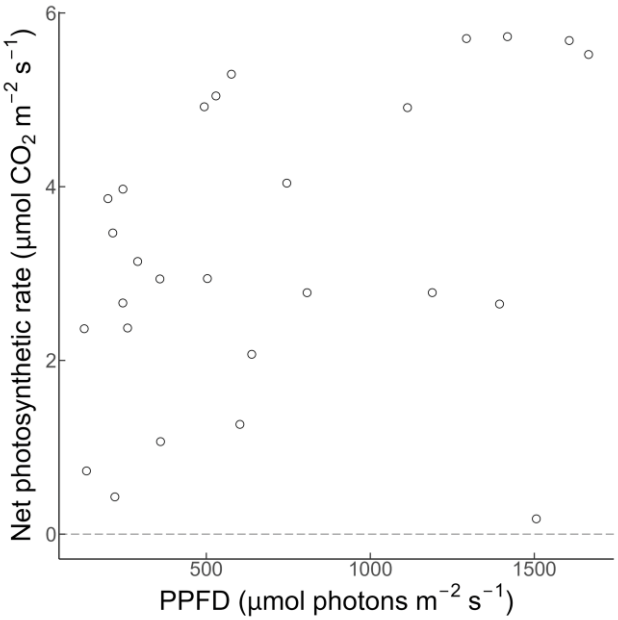

Figure 5. No clear relationship found between PPFD and NP *in situ* (NLS, n = 27, R^2_{eq} = 0.167). Measurements taken at 4.5 ± 1.5 °C and WC > 124%. Open circles show raw data.

3.2.2. Water content

WC influenced NP (QR, n =16, $F_{2, 13}$ = 18.82, R^2 = 0.704, p < 0.01; Figure 6). Data included in the regression had temperatures of 4.5 ± 1.5 °C and PPFDs greater than 480 µmol photons m^{-2} s^{-1}. The WCP was 124% and WC_{opt} was 269 ± 45%.

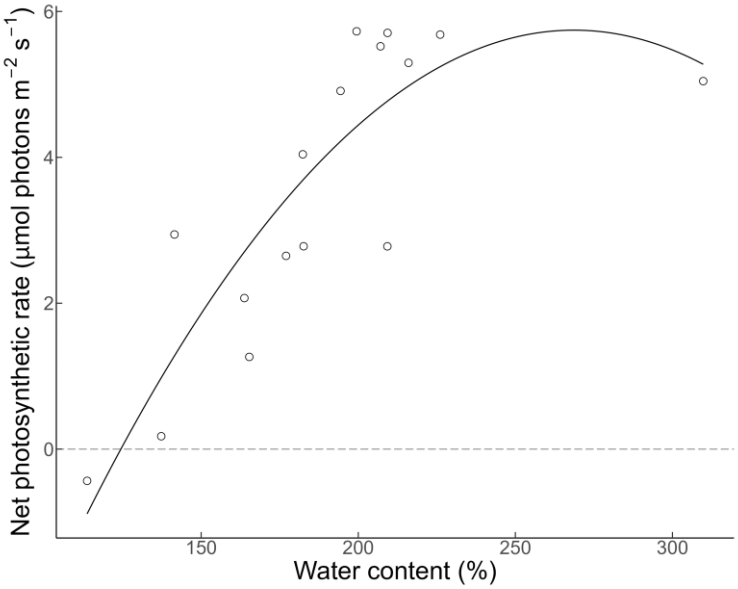

Figure 6. Water content significantly influenced *S. uncinata* NP in the field (QR, n = 16, $F_{2, 13}$ = 18.82, R^2 = 0.704, p < 0.01). Data included have PPFDs greater than 480 µmol photons m^{-2} s^{-1} and temperatures 4.5 ± 1.5 °C. WCP was 124% and WC_{opt} was 269 ± 45%. Open circles show raw data.

3.2.3. Temperature response

I did not quantify a temperature response from field data. This was due to the limited ambient temperature range during data collection.

3.3. Photosynthetic response to manipulated conditions

NP_{max} was 3.99 µmol CO_2 m^{-2} s^{-1} and occurred when PPFD was 1140 µmol photons m^{-2} s^{-1}, temperature was 10 °C, and WC was 107%.

3.3.1. Light response curves

Light influenced NP rates at all temperatures (NLS, n = 14 - 35, pseudo-R^2 = 0.957 - 0.977; Figure 7; Appendix 1).

LCPs were 34, 54, 82, and 87 µmol photons m^{-2} s^{-1} at temperatures 5, 10, 15, and 20 °C, respectively. LSPs were 480, 582, 378, and 370 µmol photons m^{-2} s^{-1} at temperatures 5, 10, 15, and 20 °C, respectively. NP_{max} at each temperature was 3.72, 3.99, 3.26, and 3.69 µmol CO_2 m^{-2} s^{-1} (Appendix 2).

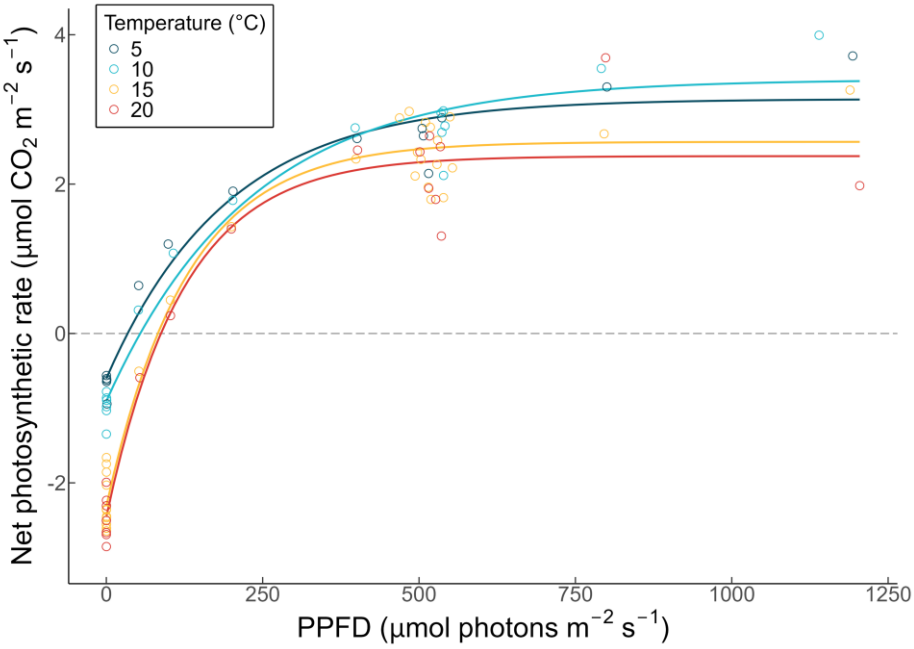

Figure 7. Light response curves at 5, 10, 15, and 20 ± 1 °C (NLS, n = 14 - 35, R^2_{eq} = 0.957 - 0.977). LCP and LSP were 34 and 480 µmol photons m^{-2} s^{-1} at 5 °C, 54 and 582 µmol photons m^{-2} s^{-1} at 10 °C, 82 and 378 µmol photons m^{-2} s^{-1} at 15 °C, and 87 and 370 µmol photons m^{-2} s^{-1} at 20 °C. Measurements taken at WC_{opt}. Open circles are raw data.

3.3.2. Water content

NP at a PPFD of 550 ± 60 µmol photons m^{-2} s^{-1} was significantly affected by WC at all temperatures tested (QR, n = 16 - 31, R^2 = 0.676 - 0.903, $F_{2, 13\text{-}27}$ = 16.61 - 80.48, $p < 0.01$;

Table 1; Figure 8). DR was also significantly impacted by WC at all temperatures tested (QR, n = 16 - 34, R^2 = 0.835 - 0.973, $F_{2, 13\text{-}30}$ = 46.56 - 428.30, $p < 0.01$; Table 1; Appendix 1).

Table 1. Quadratic regressions showed a significant relationship of water content with NP and DR at all measured temperatures.

	Temperature (± 1°C)	R^2	F statistic (df)	n	p value
NP	5	0.676	16.61 (2, 13)	16	<0.01
	10	0.903	80.48 (2, 15)	18	<0.01
	15	0.840	76.96 (2, 27)	31	<0.01
	20	0.881	56.49 (2, 13)	16	<0.01
DR	5	0.887	59.79 (2, 13)	16	<0.01
	10	0.835	46.56 (2, 16)	19	<0.01
	15	0.964	428.30 (2, 30)	34	<0.01
	20	0.973	290.10 (2, 14)	17	<0.01

The maximum, fully saturated WC was 159%. WC_{opt} was calculated to be 109 ± 17%, 119 ± 19%, 111 ± 16%, and 108 ± 15% at temperatures 5, 10, 15, and 20 °C, respectively. WCP for each temperature was 56, 59, 60, and 60% for 5, 10, 15, and 20 °C (Appendix 2).

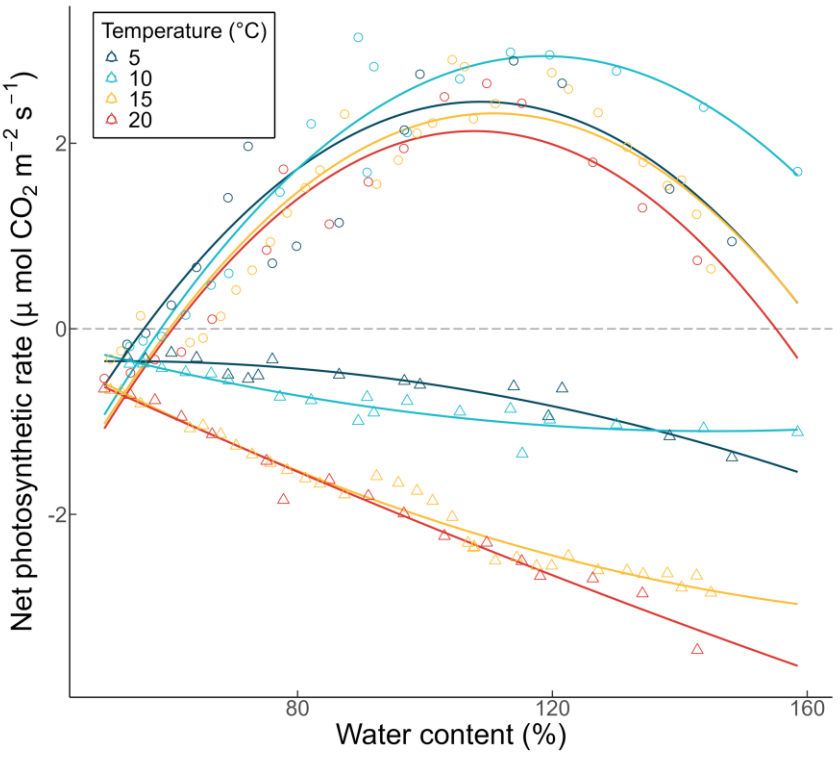

Figure 8. Water content had a significant influence on NP (open circles) and DR (triangles) at temperatures 5, 10, 15, and 20 ± 1 °C (QR, n = 16 - 31, R^2 = 0.676 - 0.903, $F_{2, 13\text{-}27}$ = 16.61 - 80.48, $p < 0.01$) as well as between WC and DR (QR, n = 16 - 34, R^2 = 0.835 - 0.973, $F_{2, 13\text{-}30}$ = 46.56 - 428.30, $p < 0.01$). PPFD was 550 ± 60 μmol photons m^{-2} s^{-1}. Points are raw data.

3.3.3. Temperature response

At WC_{opt}, there was no relationship between temperature and NP at a PPFD of 550 ± 60 µmol photons m^{-2} s^{-1} (QR, n = 27, R^2 = 0.156, $F_{2, 24}$ = 3.402, p = 0.05). Temperature did have a significant effect on DR (QR, n = 33, R^2 = 0.771, $F_{2, 30}$ = 54.82, p < 0.01; Figure 9). The Q_{10} value for DR was 3.24. Temperature response at additional PPFD levels is available in Appendix 3.

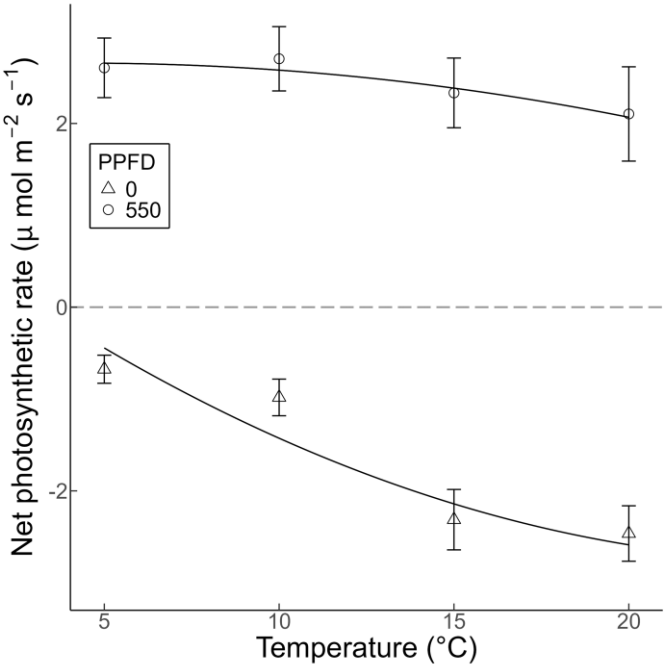

Figure 9. Impact of temperature on NP at PPFD = 550 ± 60 µmol photons m^{-2} s^{-1} (open circles) and on DR (triangles). There was no significant relationship between NP and temperature at PPFD = 550 ± 60 µmol photons m^{-2} s^{-1} (QR, n = 27, R^2 = 0.156, $F_{2, 24}$ = 3.402, p = 0.05). There was a significant influence of temperature on DR (QR, n = 33, R^2 = 0.771, $F_{2, 30}$ = 54.82, p < 0.01). Q_{10} was 3.24. Points are the mean of repeated measures on a single sample at each temperature. Error bars are one standard deviation above and below the mean. Measurements taken at WC_{opt}.

3.4. Comparing field and laboratory regressions

3.4.1. Light response curves

The regression coefficients for the field data had higher uncertainty (95% CI = [2.4, 6.0], [-2.7, 5.3], and [-8.8, -3.3], n = 27) than lab data (95% CI = [2.7, 3.6], [-0.9, -0.3], and [-5.7, -4.8], n = 15; Figure 10). CI of coefficients overlapped, suggesting that the field and laboratory light responses were comparable despite the higher noise in field measurements (Figure 10).

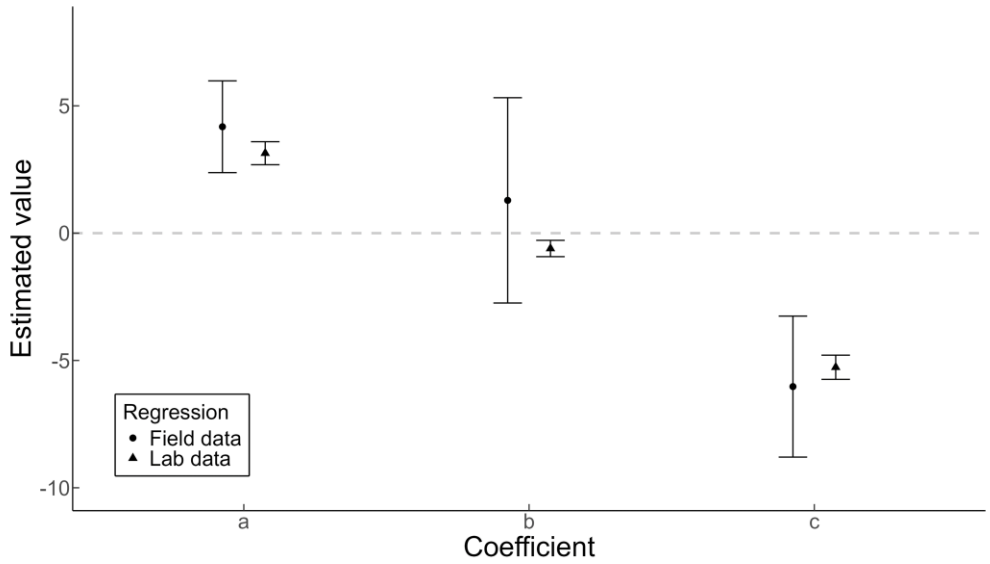

Figure 10. Comparison of estimated coefficients for NLS light response curves. Circles show estimated values based on field data (n = 27) and triangles show estimated values based on lab data (n = 15) where temperature is 5 ± 1 °C. Error bars show the 95% confidence interval.

3.4.2. Water content

The uncertainty in field (CI = [-21.76, -6.62], [0.07, 0.22] and [-0.0004, -0.0001], n = 16) versus lab (CI = [-11.40, -4.42], [0.11, 0.27], [-0.001, 0.00], n = 16) desiccation curves was somewhat comparable. Coefficients b and c are similar and have overlapping CI. Coefficient a seems to be distinct between the two regressions (Figure 11). It is difficult to determine whether the water responses are distinct or just appear different because of the error in measurements.

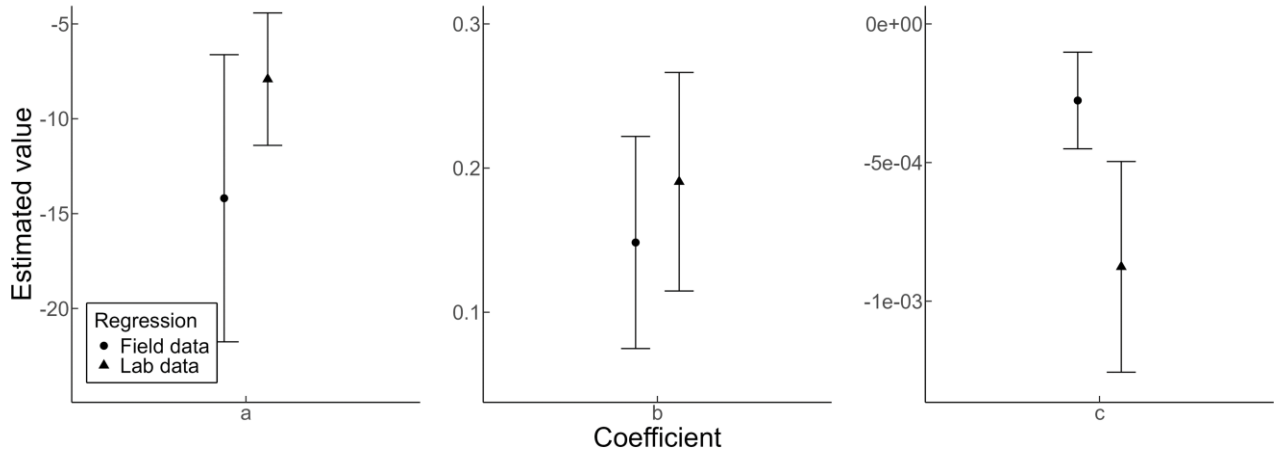

Figure 11. Comparison of estimated coefficients for quadratic regression of desiccation curve. Circles show estimated values based on field data (n = 16) and triangles show estimated values based on lab data (n = 16) where temperature is 5 ± 1 °C. Note different scales on the y-axis. Error bars two standard errors above and below the mean.

4. Discussion

The Antarctic climate is extreme, yet vegetation persists. Bryophytes are dominant because of their ability to tolerate stressful conditions and quickly respond when more favourable conditions arise. One key moss species in the maritime Antarctic is *S. uncinata*, which has been used to understand past climatic change in the Antarctic as well as to understand environmental pollutants in the ecosystem. Despite its use in various studies, there is disagreement about some of *S. uncinata*'s physiological traits and preferences. In order to best understand climatic change in the maritime Antarctic and make predictions for vegetation change, there is a need to understand the baseline preferences of this species. This study has contributed to the existing knowledge about *S. uncinata* by exploring its photosynthetic response to various environmental conditions in the field and under laboratory conditions. To do this, I considered (1) the environmental conditions that *S. uncinata* is exposed to on Robert Island during the summer, (2) what *S. uncinata*'s photosynthetic response to these conditions is *in situ*, (3) how *S. uncinata* responds to light, water, and temperature conditions beyond those experienced *in situ*, as determined in a laboratory experiment, and (4) whether field and laboratory photosynthetic responses are similar.

As I initially hypothesised, the results indicated that *S. uncinata* is rarely light limited in the field. I could only determine a distinct light response from laboratory data because the regression I calculated for the field light response did not appear to be a great fit. However, comparing the field and lab regression coefficients indicated that the regressions were similar despite higher noise in the field data. Contrary to my initial hypothesis, the field data indicated that water limitation was an issue for *S. uncinata* at Robert Island. The field sample was consistently above its WCP but rarely at its WC_{opt}. The laboratory data yielded a lower WC_{opt} than field data and it is unclear whether this is due to different methodology, physiology, or an interaction with other conditions. Comparing regression coefficients did not clarify this. Overall, WC influenced both photosynthesis and respiration in the lab. Finally, while I hypothesised that *S. uncinata* may be operating at below-optimal temperatures in the field, I found that *S. uncinata* is tolerant of a broad range of temperatures. Unlike the NP rate, DR had a significant relationship with temperature.

4.1. Light response

In a previous study by Ueno et al. (2006), *S. uncinata* has demonstrated plasticity in its light response depending on habitat. The species is known to be tolerant to high light conditions such as those found at Robert Island, which had a mean PPFD of 949 µmol photons m^{-2} s^{-1} and maximum PPFD of 1999 µmol photons m^{-2} s^{-1} over the study period. I found no distinct relationship between light and *S. uncinata* NP from the field data. Considering results from the

laboratory study, however, field conditions during daylight were consistently above the LCP and often over the LSP for *S. uncinata* at 5 °C. This suggests that *S. uncinata* is not frequently light-limited in the field during January and February. Cloudy days in the maritime Antarctic can still reach light intensities of 300 µmol photons m^{-2} s^{-1} (Schroeter et al., 1995), which is well above the LCP though below the LSP.

There was a relationship between light and NP from laboratory data at each temperature step. The LCP increased with temperature from 34 to 88 µmol photons m^{-2} s^{-1} between 5 and 20 °C. These values are similar to those determined by Nakatsubo (2002) and Uchida et al. (2002) who found the LCP to be 56 µmol photons m^{-2} s^{-1} at 10 °C and 80 µmol photons m^{-2} s^{-1} at 12 °C, respectively. The increase in LCP with temperature is expected, as respiration rate increases with temperature. As the respiration rate increases, a higher photosynthetic rate is required to compensate for the losses from respiration.

The LSP also varied between temperatures. LSP was highest (582 µmol photons m^{-2} s^{-1}) at 10 °C and lowest (370 µmol photons m^{-2} s^{-1}) at 20 °C. These values are on the lower end of the LSPs found by other studies. Uchida et al. (2002) estimated LSP to be 800 µmol photons m^{-2} s^{-1} and Ueno et al. (2006) found LSP to be between 480 and 990 µmol photons m^{-2} s^{-1}. I did not find a clear pattern to the differences in LSP at different temperatures. A study by Feng et al. (2014) found a similarly indistinct pattern in the LSP of moss crusts with increasing temperature. I was unable to estimate the error for the LSPs because I used only one sample and was not able to complete multiple light saturation curves at each temperature. Because of this I was unable to formally test if the differences in LSP at each temperature were significant.

There was no evidence of photoinhibition for the light ranges tested, consistent with the findings from Davey and Rothery (1997) and Orekhova et al. (2021). Summer light levels in the Antarctic can reach nearly 2000 µmol photons m^{-2} s^{-1}, which is higher than I was able to test in the laboratory due to limitations of the LED panel. It is possible that photoinhibition may occur under field conditions which I was not able to recreate. However, Orekhova et al. (2021) found that even after periods of lab-induced photoinhibition at light levels of 2000 µmol photons m^{-2} s^{-1}, *S. uncinata* was quick to recover when light was reduced.

The regression for the field light response did not explain a high proportion of the data (pseudo-R^2 = 0.167). Visual observation of the field light regression and laboratory light regression coefficients suggested that the underlying light responses may be similar but with a high amount of noise in the field data obscuring this.

Overall, this study supports previous research that has found *S. uncinata* to have a high tolerance for intense light. LSP and LCP varied at different temperatures, which Nakatsubo (2002), Uchida et al. (2002), and Feng et al. (2014) also found. Due to lack of replication, I was unable to determine if the differences in light responses at each temperature were significantly

different. Pannewitz et al. (2005) found that temperature significantly impacted the light response in Antarctic mosses *Bryum subrotundifolium, Bryum pseudotriquertrum*, and *Ceratodon purpureus*. However, I did not find a significant influence of temperature on NP at a PPFD of 550 ± 60 µmol photons m^{-2} s^{-1} which indicates that temperature may not have a significant influence on the light response of *S. uncinata* (see section 4.3).

4.2. Water response

Water content in the field ranged from 114% to 310%. This was frequently over the sample's WCP but rarely at its WC_{opt}. This suggests that the sample was likely water limited for much of the field season. Removing the field sample from its substrate may have influenced these results. Once it had been removed, it tended to be drier than the surrounding moss. Thus, the WC indicated by this study may be lower than they would be in regular field conditions.

The water response initially seemed different in the laboratory versus the field. In the lab, the WCP and WC_{opt} were much lower at all temperatures than those calculated from field data. A field study by Nakatsubo (2002) determined that *S. uncinata* had a broad WC_{opt} between 280% and 690% in the maritime Antarctic. Uchida et al. (2002) also found a relatively high WC_{opt} of 270% to 400% for *S. uncinata* in the high Arctic. These values align somewhat with my field WC_{opt} of 269 ± 45% but are much higher and broader than my lab WC_{opt} of 109 ± 17% at 5 ± 1 °C. This difference in results may be due to methodological differences. Nakatsubo (2002), Uchida et al. (2002), and the field component of this study did not shake samples to remove excess water before taking CO_2 exchange measurements. As a result, these measurements of WC may all be higher due to excess water held on the moss surface.

Previous study by Uchida et al. (2002) and Nakatsubo (2002) have disagreed about the WCP. Uchida et al. (2002) found it to be 40% while Nakatsubo (2002) found it to be 160%. My field WCP was 124% and lab WCP was 56% at 5 ± 1 °C. Differences among the results may be due to the different tools used, which may have had varying resolutions.

While the field and lab regressions initially seemed different, comparing the model coefficients for field and laboratory regressions showed that the models are fairly similar. There is overlap between most coefficient error bars. The error associated with field measurements was high and the error of lab measurements was nearly equally high. Only one model coefficient showed no overlap between the regressions. The difference in regressions could be because the samples were acclimated to different water conditions. *S. uncinata* from wet versus dry sites show different light responses, NP_{max}, Q_{10} values, and temperature optima (Davey and Rothery, 1997; Ueno et al., 2002). Lab and field samples were from the same area, but microhabitat conditions vary on fine scales (Kennedy, 1993). Overall, the examining the model coefficients

shows that the models are relatively similar, but it is difficult to draw a single conclusion from them.

4.3. Temperature response

There was no clear relationship between temperature and NP in the laboratory at WC_{opt} and a PPFD of 550 ± 60 µmol photons m^{-2} s^{-1}. The p-value for this regression was on the threshold for significance, however, so additional data or an alternative statistical approach may yield different results. Importantly, the LSP at 10 °C is 582 µmol photons m^{-2} s^{-1}, so the NP rates measured at 10 °C may have been light-limited. Both Nakatsubo (2002) and Uchida et al. (2002) also found a relatively stable temperature response in their studies of *S. uncinata* between temperatures 5 to 15 °C (PPFD = 600 ± 50 µmol photons m^{-2} s^{-1}) and 7 to 23 °C (PPFD = 800 ± 30 µmol photons m^{-2} s^{-1}), respectively. Uchida et al. (2002) noted a decline in NP at temperatures under 7 °C. This decline was not evident in my results. However, the minimum temperature I measured in the lab was 5 °C and it is possible that NP rates may decline below this point. In contrast, Davey and Rothery (1997) found the ideal temperature for *S. uncinata* NP to be 15 to > 20 °C and Perera-Castro et al. (2020) found the ideal temperature to be 24 °C. These results were not supported by my results, but this may be due to methodological differences. Soil and moss thallus temperatures can be very different from ambient air temperatures due to radiative warming (Convey et al., 2018; Perera-Castro et al., 2020). Davey and Rothery (1997) and Perera-Castro et al. (2020) both used temperatures from within the moss bed whereas Nakatsubo (2002), Uchida et al. (2002), and myself considered air temperatures only.

Another consideration is that the PPFD level can strongly influence temperature response (Green et al., 2011). I analysed the temperature response at 550 ± 60 µmol photons m^{-2} s^{-1} because it was above the LSP at most temperatures. I also had the highest number of data points in this light range and could include an estimate of error. Analysing data at a higher or lower PPFD may illustrate a stronger temperature response. Temperature response curves at additional PPFD levels are available in Appendix 3.

There was a relationship between temperature and rates of DR, with a Q_{10} value of 3.24. This is comparable to values found by Davey and Rothery (1997), Nakatsubo (2002), and Uchida et al. (2002), which ranged from 1.99 to 3.52. Stable NP rates despite DR rates that increase with temperature suggest that the increase in gross photosynthesis with temperature is comparable to the temperature-driven rate of increase of DR.

4.4. Limitations

The primary limitation of this study is the sample size. Only one sample was used each for field and laboratory components, with data generated by taking repeat measurements on each of the samples. Because there are no replicates, this data cannot be used to draw conclusions about the *S. uncinata* population at Robert Island as a whole, or the species as a whole. The laboratory component of this study is indicative of that single sample's response to the tested conditions, and the field component is indicative of that single sample's response to the field conditions. I have drawn a comparison between the two as an indication of how photosynthetic responses in the lab versus in the field may compare, but any differences or similarities may simply be due to variations in the samples themselves. Generally, though, I would expect the genetic variation between the two samples to be low because mosses at higher latitudes primarily reproduce asexually (Smith and Convey, 2002; Block et al, 2009). Populations in the maritime Antarctic have been demonstrated to have low genetic diversity (Hebel et al., 2018). Differences between the two samples would be likely be caused by phenotypical differences rather than genetic ones. Regardless, replication would allow for broader conclusions. Sample sizes of at least three have been typical for similar studies of *S. uncinata*'s NP response to environmental conditions (Nakatsubo, 2002; Uchida et al., 2002; Ueno et al., 2006).

Another limitation is that air temperature can be a poor indicator of microhabitat temperature (Convey, 2006; Convey et al., 2018; Hrbáček et al., 2020). Vegetation distributions at higher latitudes are dependent more on microclimatic conditions than macroclimatic ones (Green et al., 2011). Air temperature measurements in the field were taken from the Risopatrón base rather than at the original location of the sample but temperature of the sample canopy itself may have been a more accurate measure. In more southern locations, ground surface temperature is driven primarily by incoming radiation rather than air temperature (Hrbáček et al., 2020). Variation in soil temperatures is also driven by albedo, insulation by snow and vegetation, and soil water content (Convey et al., 2018). Differences in canopy temperature and air temperature are driven by solar radiation and wind speed (Perera-Castro et al., 2020). These differences are most apparent on clear days and can drive *S. uncinata* canopy temperature to 34.2 °C (Perera-Castro et al., 2020). Therefore, the field sample may have been functioning at a higher temperature than the air temperature indicated.

A few additional limitations may have influenced my results. Firstly, I did not account for CO_2 fertilization. Mean ambient CO_2 was comparable between field and lab conditions at 447 and 479 ppm, respectively. Because of this, I would not expect differences in CO_2 concentration to have influenced my results greatly. Additionally, there is some uncertainty in considering NP rates in terms of moss area. Other studies have typically considered NP per unit of dry weight (Nakatsubo, 2002; Uchida et al., 2002; Ueno et al., 2006). However, this method can be inconsistent because of the variable amount of non-photosynthetic material that may be

included in measurements (Davey and Rothery, 1997). Because of the different units used, I was not able to directly compare NP rates to prior studies. Measurements of NP per unit area are known to be biased against species with low phytomass per unit area (Davey and Rothery, 1997), however I did not make comparisons with other species and so this did not impact my results. This effect should be considered by future studies if making comparisons between species.

4.5. Recommendations for future research

An immediate area of future research would be to use a larger sample size to draw broader conclusions. A minimum sample size of three would increase confidence in population- and species-level conclusions. This would improve the ability to predict future dynamics of *S. uncinata* on Robert Island and in the maritime Antarctic. Additionally, future research should consider using thallus temperature rather than air temperature and explore a wider range of temperatures than was completed in this study. Other studies have indicated ideal temperatures greater than 20 °C (Davey and Rothery, 1997) and *in situ* thallus temperatures of up to 34 °C (Perera-Castro et al., 2020). To draw conclusions specific to Robert Island and the maritime Antarctic, I would recommend an increased focus on microclimatic conditions and variations at the study site.

This study also did not consider the ability of *S. uncinata* to acclimate to different temperatures. The ability of Antarctic mosses to adjust to temperature changes has been demonstrated by Gemal et al. (2022) and Beltran-Sanz et al. (2023). As there is disagreement about the ideal temperatures for *S. uncinata* productivity, it is difficult to make predictions about how warming or cooling temperatures could influence its prevalence in the maritime Antarctic. Establishing its temperature response would be a first step to clarifying this, but as there is known plasticity in thermal responses in mosses. Understanding the acclimation potential of *S. uncinata* would improve predictions of the species' response to environmental change.

Another area of future research would be to look at the interaction specifically between light response and WC. I did not measure this interaction in this study, but Ueno et al. (2006) showed a difference in *S. uncinata* light responses depending on habitat water conditions. More generally, the phenotypic variation of *S. uncinata* is an area of future interest. The species is widespread, and its success is likely related to its tolerance for a wide range of conditions (Smith, 1999). Other species such as *Bryum argenteum* and *Ceratodon purpureus* show plasticity in morphological traits depending on environmental conditions (Wang et al., 2019; Beltrán-Sanz et al., 2023). Understanding the plasticity of *S. uncinata* traits would allow for better predictions of ecological change in the maritime Antarctic and provide a more comprehensive understanding of the species.

5. Conclusion

Due limited and conflicting conclusions from previous research, the primary aim of this study was to investigate the photosynthetic response of *S. uncinata* to changes in the three primary factors which determine moss growth: light, water, and temperature. This was done by exploring NP rates in the field at Robert Island in Maritime Antarctica and under experimental conditions in the lab. Firstly, this study has supported other research which has found that *S. uncinata* is very tolerant of high light. The samples showed no evidence of photoinhibition in the field and lab. Secondly, *S. uncinata* showed a strong preference for being within its WC_{opt} range, with NP declining quickly when it was oversaturated in the lab. However, *S. uncinata* was never oversaturated in the field. Water appears to be the primary limiting factor for this species at Robert Island. WC was often above the WSP but rarely within the WC_{opt} under field conditions. The projected increase in liquid precipitation over the Maritime Antarctic may therefore benefit the productivity of *S. uncinata*. Finally, there was no clear relationship between temperature and NP, but there was a significant increase in DR with temperature. This suggests the *S. uncinata* is able to compensate for higher respiration by equivalently increasing its gross photosynthesis over the temperature range I explored. I would expect the species to be resilient to future warming in the maritime Antarctic.

References

Baty, F., Ritz, C., Charles, S., Brutsche, M., Flandrois, J.P., and Delignette-Muller, M.L. (2015). A toolbox for nonlinear regression in R: The package nlstools. *Journal of Statistical Software*, **66**(5), pp. 1-21.

Beltrán-Sanz, N., Raggio, J., Pintado, A., Dal Grande, F., and Sancho, L.G. (2023). Physiological plasticity as a strategy to cope with harsh climatic conditions: Ecophysiological meta-analysis of the cosmopolitan moss *Ceratodon purpureus* in the Southern Hemisphere. *Plants,* **12**(3).

Benavent-González, A., Delgado-Baquerizo, M., Fernández-Brun, L., Singh, B.K., Maestre, F.T., and Sancho, L.G. (2018). Identity of plant, lichen and moss species connects with microbial abundance and soil functioning in maritime Antarctica. *Plant and Soil*, **429**, pp. 35-52.

Bindschadler, R., Vornberger, P., Fleming, A., Fox, A., Mullins, J., Binnie, D., Paulsen, S.J., Granneman, B., and Gorodetzky, D. (2008). The Landsat image mosaic of Antarctica. *Remote Sensing of Environment*, **112**, pp. 4213-4226.

Block, W., Lewis Smith, R.I., and Kennedy, A.D. (2009). Strategies of survival and resource exploitation in the Antarctic fellfield ecosystem. *Biological Reviews*, **84**(3), pp. 449-484.

Bromwich, D., Nicolas, J., Monaghan, A. Lazzara, M.A., Keller, L.M., Weidner, G.A., and Wilson, A.B. (2013). Central West Antarctica among the most rapidly warming regions on Earth. *Nature Geoscience*, **6**, pp. 139-145.

Caemmerer, S. and Farquhar, G.D. (1981). Some relationships between the biochemistry of photosynthesis and the gas exchange of leaves. *Planta*, **153**(4), pp. 376-387.

Câmara, P.E.A.S., Carvalho-Silva, M., and Stech, M. (2021). Antarctic bryophyte research—current state and future directions. *Bryophyte Diversity and Evolution*, **43**(1), pp. 221-233.

Cannone, N., Binelli, G., Worland, M. R., Convey, P., and Guglielmin, M. (2012). CO_2 fluxes among different vegetation types during the growing season in Marguerite Bay (Antarctic Peninsula). *Geoderma*, **189**, pp. 595-605.

Choi, H.B., Lim, H.S., and Yoon, Y.J. (2022). Impact of anthropogenic inputs on Pb content of moss *Sanionia uncinata* (Hedw.) Loeske in King George Island, West Antarctica revealed by Pb isotopes. *Geosciences Journal*, **26**, pp. 225-234.

Clem, K.R., Fogt, R.L., Turner, J., Lintner, B.R., Marshall, G.J., Miller, J.R., and Renwick, J.A. (2020). Record warming at the South Pole during the past three decades. *Nature Climate Change*, **10**, pp. 762-770.

Convey, P. (2006). Antarctic Climate Change and its Influences on Terrestrial Ecosystems. In: *Trends in Antarctic Terrestrial and Limnetic Ecosystems* (eds. D.M. Bergstrom, P. Convey, and A.H.L. Huiskes) pp. 253-272. Springer, Dordrecht.

Convey, P., Coulson, S.J., Worland, M.R., and Sjöblom, A. (2018). The importance of understanding annual and shorter-term temperature patterns and variation in the surface levels of polar soils for terrestrial biota. *Polar Biology*, **41**, pp. 1587-1605.

da Silva Fernandes, A., Brito, L.B., Oliveira, G.A.R., Rerraz, E.R.A., Evangelista, H., Mazzei, J.L., and Felzenszwalb, I. (2019). Evaluation of the acute toxicity, phototoxicity and embryotoxicity of a residual aqueous fraction from extract of the Antarctic moss Sanionia uncinata. *BMC Pharmacology and Toxicology*, **20**.

Davey, M.C. and Rothery, P. (1996). Seasonal variation in respiratory and photosynthetic parameters in three mosses from the Maritime Antarctic. *Annals of Botany*, **78**, pp. 719-728.

Davey, M.C. and Rothery, P. (1997). Interspecific variation in respiratory and photosynthetic parameters in Antarctic bryophytes. *New Phytologist*, **137**, pp. 231-240.

Feng, W., Zhang, Y., Wu, B., Qin, S. and Lai, Z. (2014). Influence of environmental factors on carbon dioxide exchange in biological soil crusts in desert areas. *Arid Land Research and Management*, **28**(2), pp. 186-196.

Fowbert, J.A. (1996). An experimental study of growth in relation to morphology and shoot water content in maritime Antarctic mosses. *New Phytologist*, **133**(2), pp. 363-373.

Gemal, E.L. (2021). *Variable thermal acclimation responses of net photosynthesis and respiration in moss* Bryum argenteum *var* muticum. Undergraduate dissertation. Edinburgh University. (Accessed: 13 April 2024).

Gemal, E.L., Green, T.G.A., Cary, S.C., and Colesie, C. (2022). High resilience and fast acclimation processes allow the Antarctic moss *Bryum argenteum* to increase its carbon gain in warmer growing conditions. *Biology*, **11**(12).

Green, T.G.A., Sancho, L.G., Pintado, A. and Schroeter, B. (2011). Functional and spatial pressures on terrestrial vegetation in Antarctica forced by global warming. *Polar Biology*, **34**, pp. 1643-1656.

Google Earth (2024). *Google Earth Pro* (Version 7.3.6.9796) [Computer program]. Available from: https://www.google.com/earth/about/ (Accessed 8 April 2024).

Hebel, I., Rüdinger, M.C.D., Jaña, R.A., and Bastias, J. (2018). Genetic structure and gene flow of moss *Sanionia uncinata* (Hedw.) Loeske in maritime Antarctica and southern-Patagonia. *Frontiers in Ecology and Evolution*, **6**.

Hedenäs, L. (2003). The European species of the Calliergon-Scorpidium-Drepanocladus complex, including some related or similar species. *Meylania*, **28**, pp. 1-116.

Hrbáček, F., Cannone, C., Kňažková, M., Malfasi, F., Convey, P., and Guglielmin, M. (2020). Effect of climate and moss vegetation on ground surface temperature and the active layer among different biogeographical regions in Antarctica. *Catena*, **190**.

Kandemir, R., Demir, Y., Şen, C., and Yağcioğlu, U.C. (2023). The petrogenesis of analcime in the Coppermine Formation on Robert Island, South Shetland Islands, Antarctica. *Turkish Journal of Earth Sciences*, **32**(8), pp. 961-974.

Kennedy, A.D. (1993). Water as a limiting factor in the Antarctic terrestrial environment: A biogeographical synthesis. *Arctic and Alphine Research*, **25**(4), pp. 308-315.

King, J.C., Turner, J., Marshall, G.J., Connolley, W.M. and Lachlan-Cope, T.A. (2003). Antarctic Peninsula climate variability and its causes as revealed by analysis of instrumental records. In: *Antarctic Peninsula Climate Variability: Historical and Paleoenvironmental Perspectives* (eds. E. Domack, A. Levente, A. Burnet, R. Bindschadler, P. Convey and M. Kirby) pp. 17-30. American Geophysical Union, Washington DC.

Longton, R.E. (1967) Vegetation in the maritime Antarctic. *Philosophical Transactions of the Royal Society of London. Series B, Biological Sciences*, **252**(777), pp. 213-235.

Matsuoka, K., Skoglund, A., and Roth, G. (2018). 'Quantarctica.' Available from: https://doi.org/10.21334/npolar.2018.8516e961

Mayewski, P.A., Meredith, M.P., Summerhayes, C.P., Turner, J., Worby, A., Barrett, P.J., Casassa, G., Bertler, N.A.N., Bracegirdle, T., Naveira Garabato, A.C., Bromwich, D., Campbell, H., Hamilton, G.S., Lyons, W.B., Maasch, K.A., Aoki, S., Xiao, C., and van Ommen, T. (2009). State of the Antarctic and Southern Ocean climate system. *Reviews of Geophysics*, **47**.

Mendonça, E.S., La Scala, N., Panosso, A.R., Simas, F.N.B., Schaefer, C.E.G.R. (2011). Spatial variability models of CO2 emissions from soils colonized by grass (*Deschampsia antarctica*) and moss (*Sanionia uncinata*) in Admiralty Bay, King George Island. *Antarctic Science,* **23**(1), pp. 27-33.

Mieczan, T., and Adamczuk, M. (2015). Ecology of testate amoebae (Protists) in mosses: Distribution and relation of species assemblages with environmental parameters (King George Island, Antarctica). *Polar Biology*, **38**, pp. 221-230.

Nakatsubo, T. (2002). Predicting the impact of climatic warming on the carbon balance of the moss *Sanionia uncinata* on a maritime Antarctic island. *Journal of Plant Research*, **115**, pp. 99-106.

Orekhova, A., Barták, M., Casanova-Katny, A. and Hájek, J. (2021). Resistance of Antarctic moss *Sanionia uncinata* to photoinhibition: Chlorophyll fluorescence analysis of samples from the western and eastern coasts of the Antarctic Peninsula. *Plant Biology*, **23**(4), pp. 653-663.

Pannewitz., S., Green, T.G.A., Maysek, K., Schlensog, M., Seppelt, R., Sancho, L.G., Türk, R., and Schroeter, B. (2005). Photosynthetic responses of three common mosses from continental Antarctica. *Antarctic Science*, **17**(3), pp. 341-352.

Peat, H.J., Clarke, A., and Convey, P. (2007). Diversity and biogeography of the Antarctic flora. *Journal of Biogeography*, **34**, pp. 132-146.

Perera-Castro, A.V., Waterman, M.J., Turnbull, J.D., Ashcroft, M.B., McKinley, E., Watling, J.R., Bramley-Alves, J., Casanova-Katny, A., Zuniga, G., Flexas, J., Robinson, S.A. (2020). It is hot in the sun: Antarctic mosses have high temperature optima for photosynthesis despite cold climate. *Frontiers in Plant Science,* **11**.

Prather, H.M., Casanova-Katny, A., Clements, A.F., Chmielewski, M.W., Balkan, M.A., Shortlidge, E.E., Rosenstiel, T.N., and Eppley, S.M. (2019). Species-specific effects of passive warming in an Antarctic moss system. *Royal Society Open Science*, **6**(11).

Putzke, J., Athanásio, C.G., Albuquerque, M.P., Victoria, F., and Pereira, A.B. (2015). Comparative study of moss diversity in South Shetland Islands and in the Antarctic Peninsula. *Revisita Chilena de Historia Natural*, **88**.

Putzke, J., Vieira, F.C.B., and Pereira, A.B. (2020). Vegetation recovery after the removal of a facility in Elephant Island, Maritime Antarctic. *Land Degradation & Development,* **31**(1), pp. 96-104.

Posit team (2023). *RStudio: Integrated Development Environment for R* (Version 2023.06.1) [Computer program]. Available from: http://www.posit.co/ (Accessed: 27 March 2024).

R Core Team (2021). *R: A language and environment for statistical computing* (Version 4.1.1) [Computer program]. Available from: https://www.R-project.org/ (Accessed: 27 March 2024).

Rantanen, M., Karpechko, A.Y., Lipponen, A., Nordling, K., Hyvärinen, O., Ruosteenoja, K., Vihma, T., and Laaksonen, A. (2022). The Arctic has warmed nearly four times faster than the globe since 1979. *Communications Earth and Environment*, **3**.

Robinson, S.A., Wasley, J. and Tobin, A.K. (2003). Living on the edge – plants and global change in continental and maritime Antarctica. *Global Change Biology*, **9**, pp. 1681-1717.

Robinson, D., Hayes, A., and Couch, S. (2023). broom: Convert Statistical Objects into Tidy Tibbles (Version 1.0.5). Available from: https://CRAN.R-project.org/package=broom (Accessed: 27 March 2024).

Royles, J. and Griffiths, H. (2015). Invited review: climate change impacts in polar regions: Lessons from Antarctic moss bank archives. *Global Change Biology*, **21**, pp. 1041-1057.

Royles, J., Ogée, J., Wingate, L., Hodgson, D.A., Convey, P. and Griffiths, H. (2012). Carbon isotope evidence for recent climate-related enhancement of CO_2 assimilation and peat accumulation rates in Antarctica. *Global Change Biology*, **18**, pp. 3112-3124.

Schabenberger, O. and Pierce, F.J. (2001). *Contemporary Statistical Models for the Plant and Soil Sciences* (1st ed.). CRC Press, Boca Raton.

Schlensog, M., Green, T.G.A., Schroeter, B. (2013). Life form and water source interact to determine active time and environment in cryptogams: an example from the maritime Antarctic. *Oecologia*, **173**, pp. 59-72.

Schneider, C.A., Rasband, W.S., and Eliceiri, K.W. (2012). NIH Image to ImageJ: 25 years of image analysis. *Nature Methods*, **9**(7), pp. 671-675.

Schroeter, B., Olech, M., Kappen, L., and Heitland, W. (1995). Ecophysical investigations of *Usnea antarctica* in the maritime Antarctic: I. Annual microclimatic conditions and potential primary production. *Antarctic Science*, **7**(3), pp. 251-260.

Schroeter, B., Green, T.G.A., Kulle, D., Pannewitz, S., Schlensog, M., and Sancho, L.G. (2012). The moss *Bryum argenteum* var. *muticum* Brid. is well adapted to cope with high light in continental Antarctica. *Antarctic Science,* **24**(3), pp. 281-291.

Secretariat of the Antarctic Treaty (2012). *Antarctic Specially Protected Area No 112 (Coppermine Peninsula, Robert Island, South Shetland Islands): Revised Management Plan*. ARCM XXXV-CEP XV Hobart. Available from: https://www.ats.aq/devAS/Meetings/Measure/503 (Accessed: 14 April 2024).

Silva, D.C., Moura, T.S., D'Oliveira-Matielo, C.B., Stefenon, V.M. (2018). Antarctic mosses: Ecology and survival in the most inhospitable environment on the planet. In: *Mosses: Ecology, life cycle, and significance* (eds. O.S. Pokrovsky, I. Volkova, N. Kosykh, and V. Shevchenko) pp. 253-273. Nova Science Publishers, New York.

Smellie, J.L., Pankhurst, R., Thomson, M.R.A., and Davies, R.E.S. (1984). *The geology of the South Shetland Islands: VI. Stratigraphy, geochemistry, and evolution.* British Antarctic Survey, Cambridge.

Smith, R.I.L. (1999). Biological and environmental characteristics of three cosmopolitan mosses dominant in continental Antarctica. *Journal of Vegetation Science*, **10**, pp. 231-242.

Smith, R.I.L., & Convey, P. (2002). Enhanced sexual reproduction in bryophytes at high latitudes in the maritime Antarctic. *Journal of Bryology,* **24**(2), pp. 107-117.

Soetaert, K. (2009). rootSolve: Nonlinear root finding, equilibrium and steady-state analysis of ordinary differential equations (Version 1.8.2.4). Available from: https://cran.r-project.org/web/packages/rootSolve/index.html (Accessed: 14 April 2024).

Tarca, G., Guglielmin, M., Convey, P., Worland, M.R., and Cannone, N. (2022). Small-scale spatial-temporal variability in snow cover and relationships with vegetation and climate in maritime Antarctica. *CATENA*, **208**.

Turner, J., Lu, H., White, I., King, J.C., Philips, T., Hosking, J.S., Bracegirdle, T.J., Marshall, G.J., Mulvaney, R., and Deb, P. (2016). Absence of 21st century warming on Antarctic Peninsula consistent with natural variability. *Nature*, **535**, pp. 411-415.

Turner, J., Marshall, G.J., Clem, K., Colwell, S., Phillips, T., and Lu, H. (2019). Antarctic temperature variability and change from station data. *International Journal of Climatology*, **40**, pp. 2986–3007.

Uchida, M., Muraoka, H., Nakatsubo, T., Bekku, Y., Ueno, T., Kanda, H., and Koizumi, H. (2002) Net photosynthesis, respiration, and production of the moss *Sanionia uncinata* on a glacier foreland in the high Arctic, Ny- Ålesund, Svalbard. *Arctica, Antarctic, and Alphine Research*, **34**(3), pp. 287-292.

Ueno, T., Bekku, Y., Uchida, M., and Kanda, H. (2006). Photosynthetic light responses of a widespread moss, *Sanionia uncinata*, from contrasting water regimes in the high Arctic tundra, Svalbard, Norway. *Journal of Bryology*, **28**, pp. 345-349.

Vignon, É., Roussel, M.L., Gorodetskaya, I.V., Genthon, C., and Berne, A. (2021). Present and future of rainfall in Antarctica. *Geophysical Research Letters*, **48**.

Wang, L., Zhao, L., Song, X., Wang, Q., Kou, J., Jiang, Y. and Shao, X. (2019). Morphological traits of *Bryum argenteum* and its response to environmental variation in arid and semi-arid areas of Tibet. *Ecological Engineering*, **136**, pp. 101-107.

Wickham, H., Averick, M., Bryan, J., Chang, W., McGowan, L.D., François, R., Grolemund, G., Hayes, A., Henry, L., Hester, J., Kuhn, M., Pedersen, T.L., Miller, E., Bache, S.M., Müller, K., Ooms, J., Robinson, D., Seidel, D.P., Spinu, V., Takahashi, K., Vaughan, D., Wilke, C., Woo, K., and Yutani, H. (2019). Welcome to the tidyverse. *Journal of Open Source Software*, **4**(43).

Wu, Q., Wang, X., and Zhou, Q. (2014) Biomonitoring persistent organic pollutants in the atmosphere with mosses: Performance and application. *Environment International*, **66**, pp. 28-37.

Appendices

Appendix 1. Model summary tables

1.1. Regressions from laboratory data

Table A.1.1. Summary of model output for lab light response curves at all measured temperatures. P value indicates whether the coefficient is significantly different from 0. Coefficients from a NLS regression where $NP = a + (b - a) * e^{-e^{c} * PPFD}$

Temperature (± 1°C)	Pseudo R^2	n	Coefficient	Estimate	95% CI	p
5	0.965	15	a	3.14	2.69, 3.59	<0.01
			b	-0.60	-0.92, -0.28	<0.01
			c	-5.27	-5.74, -4.79	<0.01
10	0.967	17	a	3.40	2.84, 3.96	<0.01
			b	-0.91	-1.22, -0.59	<0.01
			c	-5.44	-5.89, -4.98	<0.01
15	0.977	35	a	2.57	2.33, 2.80	<0.01
			b	-2.31	-2.51, -2.12	<0.01
			c	-4.85	-5.17, -4.53	<0.01
20	0.957	19	a	2.37	1.96, 2.79	<0.01
			b	-2.46	-2.86, -2.05	<0.01
			c	-4.81	-5.28, -4.34	<0.01

Table A.1.2. Summary of model output for lab desiccation curves at all measured temperatures where PPFD = 550 ± 60 µmol photons m^{-2} s^{-1}. P value indicates model significance and coefficient p value indicates whether the coefficient is significantly different from 0. Coefficients from a quadratic regression where $NP = a + b(WC) + c(WC)^2$

Temperature (± 1°C)	R^2	p	n	Coefficient	Estimate	CI	Coefficient p
5	0.676	<0.01	16	a	-7.91	-11.40, -4.42	<0.01
				b	0.19	0.11, 0.27	<0.01
				c	-0.001	-0.001, 0.00	<0.01
10	0.903	<0.01	18	a	-8.49	-10.31, -6.67	<0.01
				b	0.19	0.15, 0.23	<0.01
				c	-0.001	-0.001, -0.001	<0.01
15	0.840	<0.01	31	a	-8.68	-10.51, -6.83	<0.01
				b	0.20	0.16, 0.24	<0.01
				c	-0.001	-0.001, -0.001	<0.01
20	0.881	<0.01	16	a	-8.91	-11.07, -6.74	<0.01
				b	0.20	0.16, 0.25	<0.01
				c	-0.001	-0.001, -0.001	<0.01

Table A.1.3. Summary of model output for lab desiccation curves at all measured temperatures where PPFD = 0 µmol photons m^{-2} s^{-1}. Overall p value indicates model significance and coefficient p value indicates whether the coefficient is significantly different from 0. Coefficients from a quadratic regression where $NP = a + b(WC) + c(WC)^2$

Temperature (± 1°C)	R^2	p	n	Coefficient	Estimate	CI	Coefficient p
5	0.887	<0.01	16	a	-0.64	-1.30, 0.02	0.07
				b	0.011	0.00, 0.03	0.15
				c	-0.0001	-0.0001, 0.00	0.01
10	0.835	<0.01	19	a	0.80	0.25, 1.35	0.01
				b	-0.03	-0.04, -0.01	<0.01
				c	0.0001	0.00, 0.0001	<0.01
15	0.964	<0.01	34	a	1.42	0.86, 1.99	<0.01
				b	-0.05	-0.06, -0.03	<0.01
				c	0.0001	0.00, 0.0002	<0.01
20	0.973	<0.01	17	a	0.99	0.22, 1.77	0.02
				b	-0.03	-0.05, -0.02	<0.01
				c	-0.00003	-0.0001, 0.0001	0.50

Table A.1.4. Summary of model output for lab temperature response curves where PPFD = 0 µmol photons m^{-2} s^{-1} and 550 ± 60 µmol photons m^{-2} s^{-1}. Overall p value indicates model significance and coefficient p value indicates whether the coefficient is significantly different from 0. Coefficients from a quadratic regression where $NP = a + b(temp) + c(temp)^2$

PPFD (µmol photons m^{-2} s^{-1})	R^2	p	n	Coefficient	Estimate	95% CI	Coefficient p
0	0.771	<0.01	33	a	0.81	-0.05, 1.66	0.07
				b	-0.28	-0.42, -0.13	<0.01
				c	0.01	-0.0002, 0.01	0.06
550 ± 60	0.156	0.05	27	a	2.61	1.64, 3.58	<0.01
				b	0.02	-0.14, 0.18	0.20
				c	-0.002	-0.01, 0.004	0.46

1.2. Regressions from field data

Table A.1.5. Summary of model output for field light response curve. P value indicates whether the coefficient is significantly different from 0. Coefficients from a NLS regression where $NP = a + (b - a) * e^{-e^{c} * PPFD}$

Temperature (± 1.5 °C)	Pseudo R^2	n	Coefficient	Estimate	95% CI	p
4.5	0.167	27	a	4.18	2.38, 5.98	<0.01
			b	1.29	-2.74, 5.32	0.52
			c	-6.03	-8.80, -3.26	<0.01

Table A.1.6. Summary of model output for field desiccation curves where PPFD is greater than 500 µmol photons m^{-2} s^{-1}. P value indicates model significance and coefficient p value indicates whether the coefficient is significantly different from 0. Coefficients from a quadratic regression where $NP = a + b(WC) + c(WC)^2$

Temperature (± 1.5°C)	R^2	p	n	Coefficient	Estimate	CI	Coefficient p
4.5	0.704	<0.01	16	a	-14.19	-21.76, -6.62	<0.01
				b	0.15	0.07, 0.22	<0.01
				c	-0.0003	-0.0004, -0.0001	<0.01

Appendix 2. Summary tables for calculated values

Table A.2.1. Summary of LCP, LSP, and NP_{max} for *S. uncinata* during lab measurements. Measurements taken at WC_{opt}.

Temperature (± 1°C)	LCP (µmol photons m^{-2} s^{-1})	LSP (µmol photons m^{-2} s^{-1})	NP_{max} (µmol CO_2 m^{-2} s^{-1})
5	34	480	3.72
10	54	582	3.99
15	82	378	3.26
20	87	370	3.69

Table A.2.2. Summary of WCP, WC_{opt}, and NP_{max} for *S. uncinata* during lab measurements. Measurements taken at PPFD = 550 ± 60 µmol photons m^{-2} s^{-1}.

Temperature (± 1°C)	WCP (%)	WC_{opt} (%)	NP_{max} (µmol CO_2 m^{-2} s^{-1})
5	55.9	109 ± 17	2.45
10	58.5	119 ± 19	2.94
15	59.9	111 ± 16	2.32
20	60.4	108 ± 15	2.13

Appendix 3. Complete light response curves for all PPFD levels

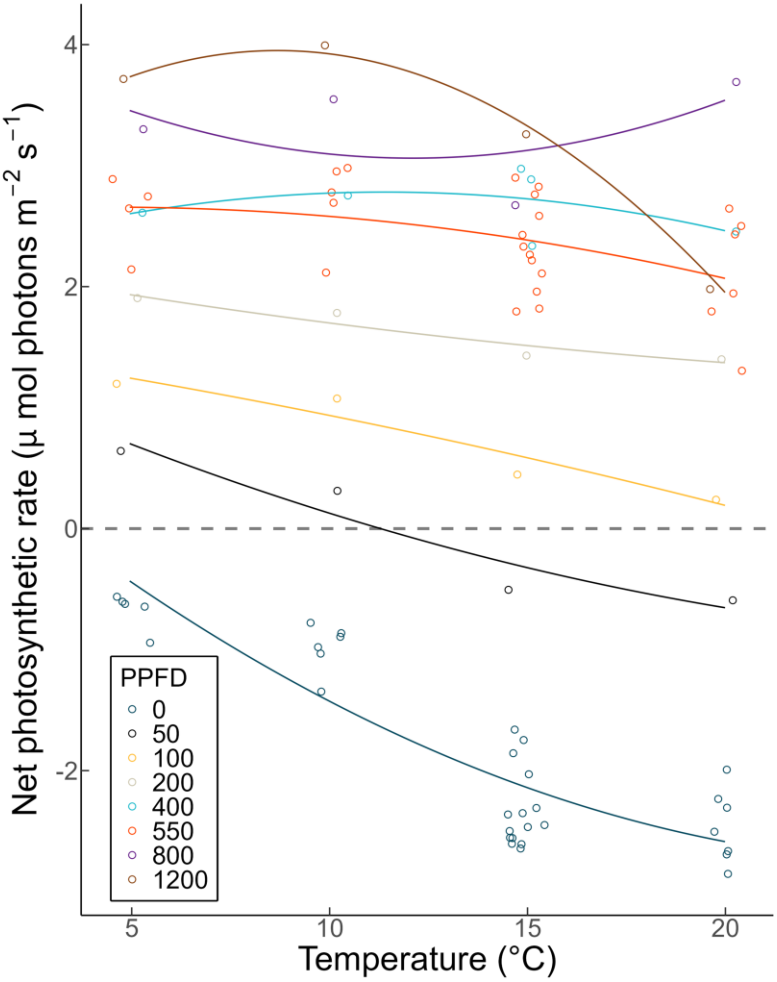

Figure A.3.1. Temperature response curves at each light intensity. Temperature response curves were not measured directly but were interpreted from data taken during other lab measurements. Points are raw data.

Appendix 4. Code and data

Full code with annotations and data available on GitHub: https://github.com/acolety/dissertation

Code excerpts below, including data filtering, models, and calculations.

```
# LOADING DATA ----
# field data
sanioniaField <- read.csv("data\\field\\sanionia.csv") %>%
  filter(Code == "MP_010")

# lab data
sanioniaLab <- read.csv("data\\lab\\sanioniaLab.csv") %>%
  filter(Object == 1)




# CREATING SUBSETS ----
## field
### light
LCfield <- sanioniaField %>%
  filter(waterContent > 124,
         between(tempWS, 3, 6))

### water content
WCfield <- sanioniaField %>%
  filter(between(tempWS, 3, 6),
         between(partop, 500, 1700))


## lab
### light
LC <- sanioniaLab %>%
  filter(between(waterContent, 93, 138) & !tempCat == 25)

#### LC dataframe for each temperature
LC5dat <- LC %>%
  filter(tempCat == 5)

LC10dat <- LC %>%
  filter(tempCat == 10)

LC15dat <- LC %>%
  filter(tempCat == 15)

LC20dat <- LC %>%
  filter(tempCat == 20)


### water content
WC <- sanioniaLab %>%
  filter(parCat %in% c(0, 550) & !tempCat == 25)

WCphotosynth <- WC %>%
  filter(partop > 5)

WCresp <- sanioniaLab %>%
  filter(partop < 5 & !tempCat == 25)
```

```
### temperature
TC <- sanioniaLab %>%
  filter(between(waterContent, 93, 138) & !tempCat == 25)

#### temperature subsets for plotting
TC0plot <- TC %>%
  filter(parCat == 0)

TC550plot <- TC %>%
  filter(parCat == 550)



# RAW DATA EXPLORATION ----
## field
### checking for correlations between variables
cor.test(sanioniaField$partop, sanioniaField$tempWS)
cor.test(sanioniaField$tempWS, sanioniaField$waterContent)
cor.test(sanioniaField$waterContent, sanioniaField$partop)

### distribution of response variable, a (NP)
hist(sanioniaField$aCorrected)


## lab
### distribution of response variable, a (NP)
hist(sanioniaLab$a)



# MODELLING ----
## field
### light
LCfieldNls <- nls(aCorrected ~ SSasymp(partop, Asym, R0, lrc), data = LCfield)

plot(nlsResiduals(LCfieldNls))
summary(LCfieldNls)
overview(LCfieldNls)
1 - ((sum(residuals(LCfieldNls)^2)) / (sum((LCfield$aCorrected - mean(LCfield$aCorrec
ted))^2)))  # psuedo R2


### water
WCfieldMod <- lm(aCorrected ~ poly(waterContent, degree = 2, raw = TRUE),
                 data = WCfield)

plot(WCfieldMod)
summary(WCfieldMod)


## lab
### light
#### table of regressions for easier plotting and calculations
LCRegressions <- LC %>%
  filter(tempCat != 25) %>%
  group_by(tempCat) %>%
  do(tidy(nls(a ~ SSasymp(partop, Asym, R0, lrc), data = .)))

#### t = 5
LC5 <- nls(a ~ SSasymp(partop, Asym, R0, lrc), data = LC5dat)
```

```
plot(residuals(LC5))
summary(LC5)
overview(LC5)
##### pseudo r2
1 - ((sum(residuals(LC5)^2)) / (sum((LC5dat$a - mean(LC5dat$a))^2)))

#### t = 10
LC10 <- nls(a ~ SSasymp(partop, Asym, R0, lrc), data = LC10dat)

plot(nlsResiduals(LC10))
summary(LC10)
overview(LC10)
1 - ((sum(residuals(LC10)^2)) / (sum((LC10dat$a - mean(LC10dat$a))^2)))

#### t = 15
LC15 <- nls(a ~ SSasymp(partop, Asym, R0, lrc), data = LC15dat)

plot(nlsResiduals(LC15))
summary(LC15)
overview(LC15)
1 - ((sum(residuals(LC15)^2)) / (sum((LC15dat$a - mean(LC15dat$a))^2)))

#### t = 20
LC20 <- nls(a ~ SSasymp(partop, Asym, R0, lrc), data = LC20dat)

plot(nlsResiduals(LC20))
summary(LC20)
overview(LC20)
1 - ((sum(residuals(LC20)^2)) / (sum((LC20dat$a - mean(LC20dat$a))^2)))


### water
#### table of regressions for easier plotting and calculations
##### photosynthesis
WCPRegressions <- WCphotosynth %>%
  filter(tempCat != 25) %>%
  group_by(tempCat) %>%
  do(tidy(lm(a ~ poly(waterContent, degree = 2, raw = TRUE), data = .)))

##### dark respiration
WCRregressions <- WCresp %>%
  group_by(tempCat) %>%
  do(tidy(lm(a ~ poly(waterContent, degree = 2, raw = TRUE), data = .)))


#### photosynthesis
##### t = 5
WC5 <-  WCphotosynth %>%
  filter(tempCat == 5)  %>%
  lm(a ~ poly(waterContent, degree = 2, raw = TRUE), data = .)

plot(WC5)
summary(WC5)

##### t = 10
WC10 <-  WCphotosynth %>%
  filter(tempCat == 10)  %>%
  lm(a ~ poly(waterContent, degree = 2, raw = TRUE), data = .)

plot(WC10)
summary(WC10)
```

```
##### t = 15
WC15 <-  WCphotosynth %>%
  filter(tempCat == 15)  %>%
  lm(a ~ poly(waterContent, degree = 2, raw = TRUE), data = .)

plot(WC15)
summary(WC15)

##### t = 20
WC20 <-  WCphotosynth %>%
  filter(tempCat == 20)  %>%
  lm(a ~ poly(waterContent, degree = 2, raw = TRUE), data = .)

plot(WC20)
summary(WC20)


#### dark respiration
##### t = 5
WCR5 <-  WCresp %>%
  filter(tempCat == 5)  %>%
  lm(a ~ poly(waterContent, degree = 2, raw = TRUE), data = .)

plot(WCR5)
summary(WCR5)

##### t = 10
WCR10 <-  WCresp %>%
  filter(tempCat == 10)  %>%
  lm(a ~ poly(waterContent, degree = 2, raw = TRUE), data = .)

plot(WCR10)
summary(WCR10)

##### t = 15
WCR15 <-  WCresp %>%
  filter(tempCat == 15)  %>%
  lm(a ~ poly(waterContent, degree = 2, raw = TRUE), data = .)

plot(WCR15)
summary(WCR15)

##### t = 20
WCR20 <-  WCresp %>%
  filter(tempCat == 20)  %>%
  lm(a ~ poly(waterContent, degree = 2, raw = TRUE), data = .)

plot(WCR20)
summary(WCR20)


### temperature
#### table of regressions for easier plotting and calculations
TCRegressions <- TC %>%
  group_by(parCat) %>%
  do(tidy(lm(a ~ poly(tcuv, degree = 2, raw = TRUE), data = .)))

##### par = 0
TC0 <-  TC %>%
  filter(parCat == 0)  %>%
```

```
  lm(a ~ poly(tcuv, degree = 2, raw = TRUE), data = .)

plot(TC0)
summary(TC0)

##### par = 50
TC50 <-  TC %>%
  filter(parCat == 50)  %>%
  lm(a ~ poly(tcuv, degree = 2, raw = TRUE), data = .)

plot(TC50)
summary(TC50)

##### par = 100
TC100 <-  TC %>%
  filter(parCat == 100)  %>%
  lm(a ~ poly(tcuv, degree = 2, raw = TRUE), data = .)

plot(TC100)
summary(TC100)

##### par = 200
TC200 <-  TC %>%
  filter(parCat == 200)  %>%
  lm(a ~ poly(tcuv, degree = 2, raw = TRUE), data = .)

plot(TC200)
summary(TC200)

##### par = 400
TC400 <-  TC %>%
  filter(parCat == 400)  %>%
  lm(a ~ poly(tcuv, degree = 2, raw = TRUE), data = .)

plot(TC400)
summary(TC400)

##### par = 550
TC550 <-  TC %>%
  filter(parCat == 550)  %>%
  lm(a ~ poly(tcuv, degree = 2, raw = TRUE), data = .)

plot(TC550)
summary(TC550)

##### par = 800
TC800 <-  TC %>%
  filter(parCat == 800)  %>%
  lm(a ~ poly(tcuv, degree = 2, raw = TRUE), data = .)

plot(TC800)
summary(TC800)

##### par = 1200
TC1200 <-  TC %>%
  filter(parCat == 800)  %>%
  lm(a ~ poly(tcuv, degree = 2, raw = TRUE), data = .)

plot(TC1200)
summary(TC1200)
```

```
## creating dataframe for lab/field model output for coefficient comparison
### coefficients for light curves from models
Regression <- c(rep("Field data", 3), rep("Lab data", 3))
parameter <- rep(c("a", "b", "c"), 2)
estimate <- c(4.1788, 1.2881, -6.0263, 3.1397, -0.6030, -5.2671)
tlower <- c(2.376404, -2.742961, -8.795165, 2.6877742, -0.9233707, -5.7422698)
tupper <- c(5.981278, 5.319116, -3.257440, 3.5915746, -0.2826472, -4.7918849)

lightComparison <- data.frame(Regression, parameter, estimate, tlower, tupper)


### coefficients for desiccation curves from models
parameter2 <- rep(c("a", "b", "c"), 2)
estimate2 <- c(-1.419e+01, 1.484e-01, -2.762e-04,
               -7.9119641, 0.1905403, -0.0008762)
se <- c(3.784e+00, 3.678e-02, 8.713e-05,
        1.7454898, 0.0378941, 0.0001900)

waterComparison <- data.frame(Regression, parameter2, estimate2, se)



# CALCULATED VALUES ----
## field
### light
#### light compensation point (LCP)
LCP.field <- function(x) {
  4.1788 + (1.2881 - 4.1788) * exp(-exp(-6.0263) * x)
}

print(uniroot(LCP.field, interval = c(0, 500))$root)

#### light saturation point (LSP)
LSP.field <- function(x) {
  (4.1788 + (1.2881 - 4.1788) * exp(-exp(-6.0263) * x)) - (0.9 * 4.1788)
}

print(uniroot(LSP.field, interval = c(0, 1250))$root)


### water
#### water compensation point (WCP)
WC.field <- function(x) {
  -1.419e+01 + (1.484e-01 * x) + (-2.762e-04 * x^2)
}

print(uniroot(WC.field, interval = c(113, 200))$root)

#### optimal water content (WCopt)
optimize(function(x)
  -1.419e+01 + (1.484e-01 * x) + (-2.762e-04 * x^2), c(200, 400), maximum = T)

uniroot.all(function(x)
  (-1.419e+01 + (1.484e-01 * x) + (-2.762e-04 * x^2)) - (0.9 *5.743526),
  c(0, 500))


## lab
### light
#### light compensation point (LCP)
```

```
##### t = 5
LC.5 <- function(x) {
  LCRegressions$estimate[1] + (LCRegressions$estimate[2]
                               - LCRegressions$estimate[1])
  * exp(-exp(LCRegressions$estimate[3]) * x)
}

print(uniroot(LC.5, interval = c(0, 500))$root)

##### t = 10
LC.10 <- function(x) {
  LCRegressions$estimate[4] + (LCRegressions$estimate[5]
                               - LCRegressions$estimate[4])
  * exp(-exp(LCRegressions$estimate[6]) * x)
}

print(uniroot(LC.10, interval = c(0, 500))$root)

##### t = 15
LC.15 <- function(x) {
  LCRegressions$estimate[7] + (LCRegressions$estimate[8]
                               - LCRegressions$estimate[7])
  * exp(-exp(LCRegressions$estimate[9]) * x)
}

print(uniroot(LC.15, interval = c(0, 500))$root)

##### t = 20
LC.20 <- function(x) {
  LCRegressions$estimate[10] + (LCRegressions$estimate[11]
                                - LCRegressions$estimate[10])

  * exp(-exp(LCRegressions$estimate[12]) * x)
}

print(uniroot(LC.20, interval = c(0, 500))$root)


#### light saturation point (LSP)
##### t = 5
LSP.5 <- function(x) {
  (LCRegressions$estimate[1] + (LCRegressions$estimate[2]
                                - LCRegressions$estimate[1])
   * exp(-exp(LCRegressions$estimate[3]) * x))
  - (0.9 * LCRegressions$estimate[1])
}

print(uniroot(LSP.5, interval = c(0, 1250))$root)

##### t = 10
LSP.10 <- function(x) {
  (LCRegressions$estimate[4] + (LCRegressions$estimate[5]
                                - LCRegressions$estimate[4])
   * exp(-exp(LCRegressions$estimate[6]) * x))
  - (0.9 * LCRegressions$estimate[4])
}

print(uniroot(LSP.10, interval = c(0, 1250))$root)

##### t = 15
LSP.15 <- function(x) {
```

```
  (LCRegressions$estimate[7] + (LCRegressions$estimate[8]
                                - LCRegressions$estimate[7])
   * exp(-exp(LCRegressions$estimate[9]) * x))
  - (0.9 * LCRegressions$estimate[7])
}

print(uniroot(LSP.15, interval = c(0, 1250))$root)

##### t = 20
LSP.20 <- function(x) {
  (LCRegressions$estimate[10] + (LCRegressions$estimate[11]
                                 - LCRegressions$estimate[10]) * exp(-exp(LCRegressio
ns$estimate[12]) * x))
  - (0.9 * LCRegressions$estimate[10])
}

print(uniroot(LSP.20, interval = c(0, 1250))$root)


### water
#### optimal water content (WCopt)
##### t = 5
optimize(function(x)
  WCPRegressions$estimate[1] + WCPRegressions$estimate[2] * x
  + WCPRegressions$estimate[3] * x^2, c(80, 160), maximum = T)

uniroot.all(function(x)

  (WCPRegressions$estimate[1] + WCPRegressions$estimate[2] * x
   + WCPRegressions$estimate[3] * x^2) - (0.9 * 2.447388), c(0, 200))

##### t = 10
optimize(function(x)
  WCPRegressions$estimate[4] + WCPRegressions$estimate[5] * x
  + WCPRegressions$estimate[6] * x^2, c(80, 160), maximum = T)

uniroot.all(function(x)

  (WCPRegressions$estimate[4] + WCPRegressions$estimate[5] * x
   + WCPRegressions$estimate[6] * x^2) - (0.9 * 2.939508), c(0, 200))

##### t = 15
optimize(function(x)
  WCPRegressions$estimate[7] + WCPRegressions$estimate[8] * x
  + WCPRegressions$estimate[9] * x^2, c(80, 160), maximum = T)

uniroot.all(function(x)

  (WCPRegressions$estimate[7] + WCPRegressions$estimate[8] * x
   + WCPRegressions$estimate[9] * x^2) - (0.9 * 2.322397), c(0, 200))

##### t = 20
optimize(function(x)
  WCPRegressions$estimate[10] + WCPRegressions$estimate[11] * x
  + WCPRegressions$estimate[12] * x^2, c(80, 160), maximum = T)

uniroot.all(function(x)
  (WCPRegressions$estimate[10] + WCPRegressions$estimate[11] * x
   + WCPRegressions$estimate[12] * x^2) - (0.9 * 2.131495), c(0, 200))
```

```
#### water compensation point (WCP)
##### t = 5
uniroot(function(x) WCPRegressions$estimate[1] + WCPRegressions$estimate[2] * x
        + WCPRegressions$estimate[3] * x^2, interval = c(0, 100))

##### t = 10
uniroot(function(x)
  WCPRegressions$estimate[4] + WCPRegressions$estimate[5] * x
  + WCPRegressions$estimate[6] * x^2, interval = c(0, 100))

##### t = 15
uniroot(function(x)
  WCPRegressions$estimate[7] + WCPRegressions$estimate[8] * x
  + WCPRegressions$estimate[9] * x^2, interval = c(0, 100))

##### t = 20
uniroot(function(x)
  WCPRegressions$estimate[10] + WCPRegressions$estimate[11] * x
  + WCPRegressions$estimate[12] * x^2, interval = c(0, 100))


#### temperature
##### Q10 value
((TCRegressions$estimate[1] + TCRegressions$estimate[2] * 20
  + TCRegressions$estimate[3] * 20^2) / (TCRegressions$estimate[1] + TCRegressions$es
timate[2] * 5 + TCRegressions$estimate[3] * 5^2))^(10 / (20-5))
```